Analyst

Accepted Manuscript

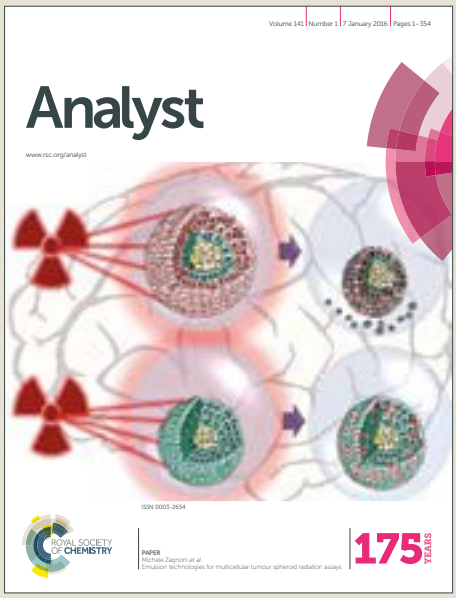

ROYAL SOCIETY OF CHEMISTRY

rsc.li/analyst

View Article Online
DOI: 10.1039/C8AN00307F

Recent Advances in Nanoparticle-based Lateral Flow Immunoassay as a Point of Care Diagnostic Tool for Infectious Agents and Diseases

Ruptanu Banerjee and Amit Jaiswal*

School of Basic Sciences, Indian Institute of Technology Mandi,

Kamand, Mandi-175005, Himachal Pradesh, India

*Corresponding Author E-mail: j.amit@iitmandi.ac.in

Abstract: Lateral Flow Immunoassay (LFIA) technology is a paper-based, point-of-care strip biosensor which are designed to detect specific analyte in a given sample. This type of assay is now of great interest to researchers for its cost-effectiveness, simplicity, portability and rapidness of detection of analytes including but not limited to areas like agriculture, food, biomedicine, pathogen detection etc. Various nanoparticles (such as metal nanoparticles, carbon-based nanoparticles, quantum dots, lanthanides, up-converting phosphor and more) functionalized by antibody to detect analyte protein or molecular marker present in surface of the infectious pathogen are been used for designing LFIA technique. Herein we review the principle of the assay and recent advancements in terms of different approaches and designs of the assay towards the detection of infectious agents and disease.

1. Introduction:

Lateral Flow (Immuno) Assay (LFIA) is the technology behind detection devices that are made for low-cost, fast and simple detection of analyte of interest in a sample of complex mixture, where the sample is placed on a test device and the results are displayed within few minutes. Originally, this technique is called "Sol Particle Immunoassay", introduced by Leuvering *et al.* in 1980 [1], however nowadays it is more commonly known as LFIA. In recent years, LFIA based diagnostic devices are being widely studied because of its low development cost and vast range of applications across multiple areas where rapid detection is a requisite. Another major advantage of LFIA-based tests is that it can be performed on a variety of biological samples

View Article Online
DOI: 10.1039/C8AN00307F

which include plasma [2], sweat [3, 4], saliva [5, 6], serum [7, 8], urine [9, 10], whole blood [11, 12], *etc.* and the quantity of sample required for detection is much lesser than that needed for conventional assays.

Since its development, LFIA has achieved penetration in a broad spectrum of market. Fig-1 depicts the application in various industries in which LFIAs are already in production or are known to be in development stages [13]. Amongst different applications of LFIA based tools, one of the major area is detecting infectious disease. Over the year, various detection methods have been implemented for fast, correct and low-cost detection of the infection causing pathogen or molecular marker associated with it e.g. antigen or proteins [14]. LFIA allows a wide range of qualitative, semi-quantitative and quantitative detection of infectious diseases caused by pathogens with high specificity and selectivity [15]. In general, disease diagnosis and its subsequent treatment or prevention heavily depends on highly skilled professionals. LFIA devices can bridge the gap between the production of highly sensitive and selective data for diagnosis of disease and minimally skilled or trained personal to produce result in a very short time.

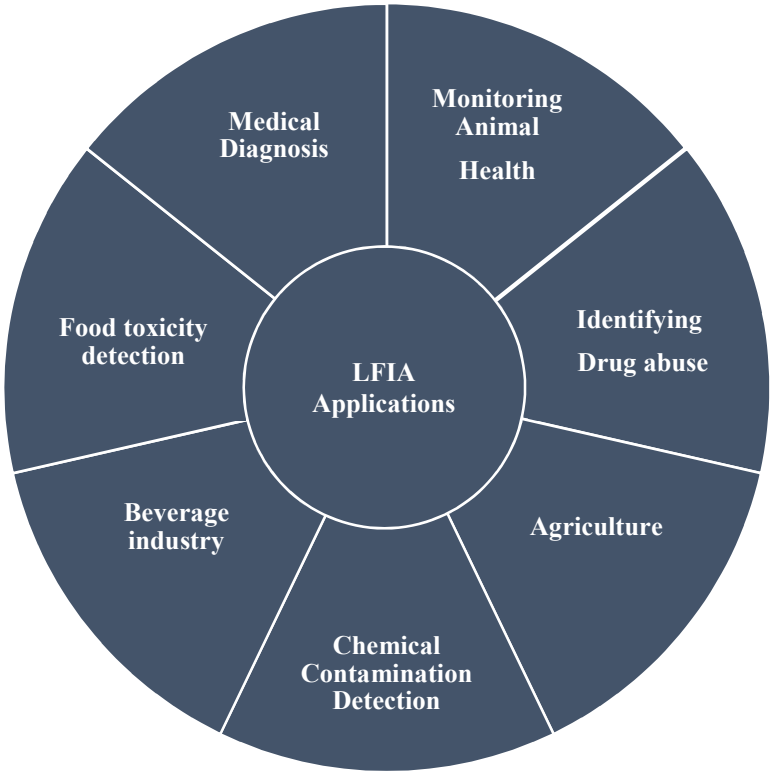

View Article Online
DOI: 10.1039/C8AN00307F

Figure-1: Market for LFIA as a POC tool or on-field technology use

In a global scenario, nearly 9 million people have died due to various infectious diseases (Tuberculosis, Gonorrhoeae, HIV/AIDS, Hepatitis, Dengue, Chikungunya to name a few) which accounts for about 15.8 % of all deaths in 2015 [16]. The diagnosis of infectious diseases is mostly laboratory based, time consuming (several days to months), requires well equipped technical facilities and highly trained technicians. It is clear that for infectious diseases, diagnostics play a valuable and critical role in the care of patients with the disease and those at risk of developing them. Early diagnostics reduces the chance of death or the severity of disease as there are various treatments available ranging from vaccination to antibacterial drug supplementation. In this scenario, point-of-care (POC) tests like LFIA emerges out to be protagonist in fulfilling the necessities of an early test that has a comparable confidence with laboratory based diagnostic methods and having the advantages of being rapid, simple, low-cost and the ability of it to be performed irrespective of a laboratory set-up or a trained person for operation.

The global risk for infectious diseases is very high and in the upcoming years, developing countries will face this as a major threat as pandemics (Fig-2) [17]. Over the past few decades, nanoparticle based lateral flow biosensors are rapidly been developed to meet the diagnostic needs for detecting infectious diseases. In the present review, we emphasize on detection of infectious diseases with nanoparticle based LFIA devices. Nanoparticles are used as a probe molecule and serve as the detection module of the LFIA device. Nanoparticles become a material of choice for probes due to its robustness, size and shape dependent tuneable opto-electrical properties, rapid synthesis and ease of functionalization, biocompatibility, persistent stability, visual signal interpretation with high signal-to-noise ratio and low developmental cost. There are several interesting reviews available for the fabrication of LFIA devices using various labels and its application towards biosensing [14, 15, 18-26]. However, only one review was published in 2010 by Ngom et. al. on application of lateral flow test strip devices on detection of infectious agents and chemical contaminants [27]. After this, several new strategies as well as improvements are implemented with new-age technology for detection of biomarkers of infectious diseases. The present review aims to provide a comprehensive collection of all the upgradation and recent trends in the detection of infectious diseases using nanoparticle based LFIA devices.

View Article Online
DOI: 10.1039/C8AN00307F

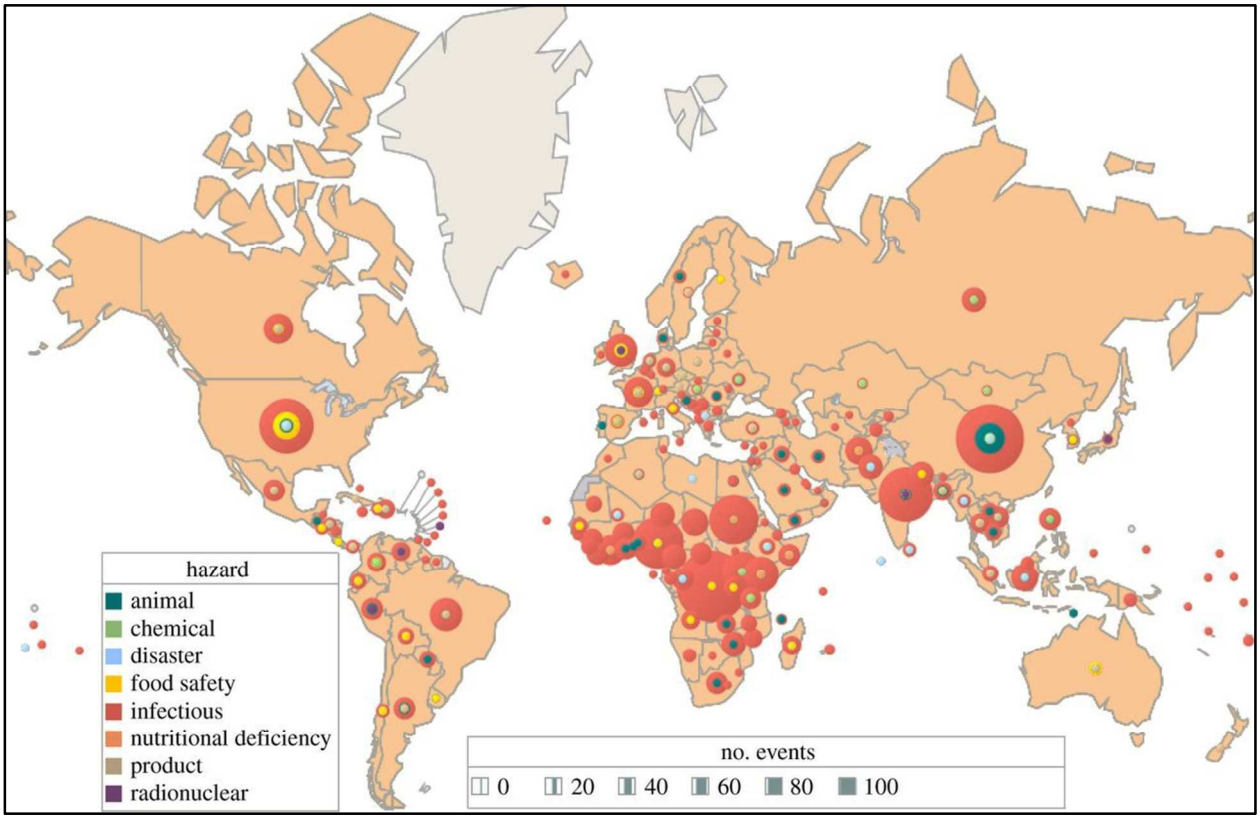

Figure-2: A total of 2797 international health hazards by type and country, January 2001–September 2013. Eighty-four per cent were outbreaks of infectious diseases. Unpublished WHO data (2013). Reprinted (adapted) with permission from [17]. Copyright (2014) The Royal Society Publishing.

2. Principle of assay

The principle behind lateral flow assay is the movement of the liquid sample or the sample containing the analyte of interest along a strip (Figure 3). The strip is made with polymeric materials and have specific zones or sites where molecules have been conjugated with a label. When the analyte containing sample passes through these zones, they interact with the molecules designed to bind specifically to the analyte present in the sample.

View Article Online
DOI: 10.1039/C8AN00307F

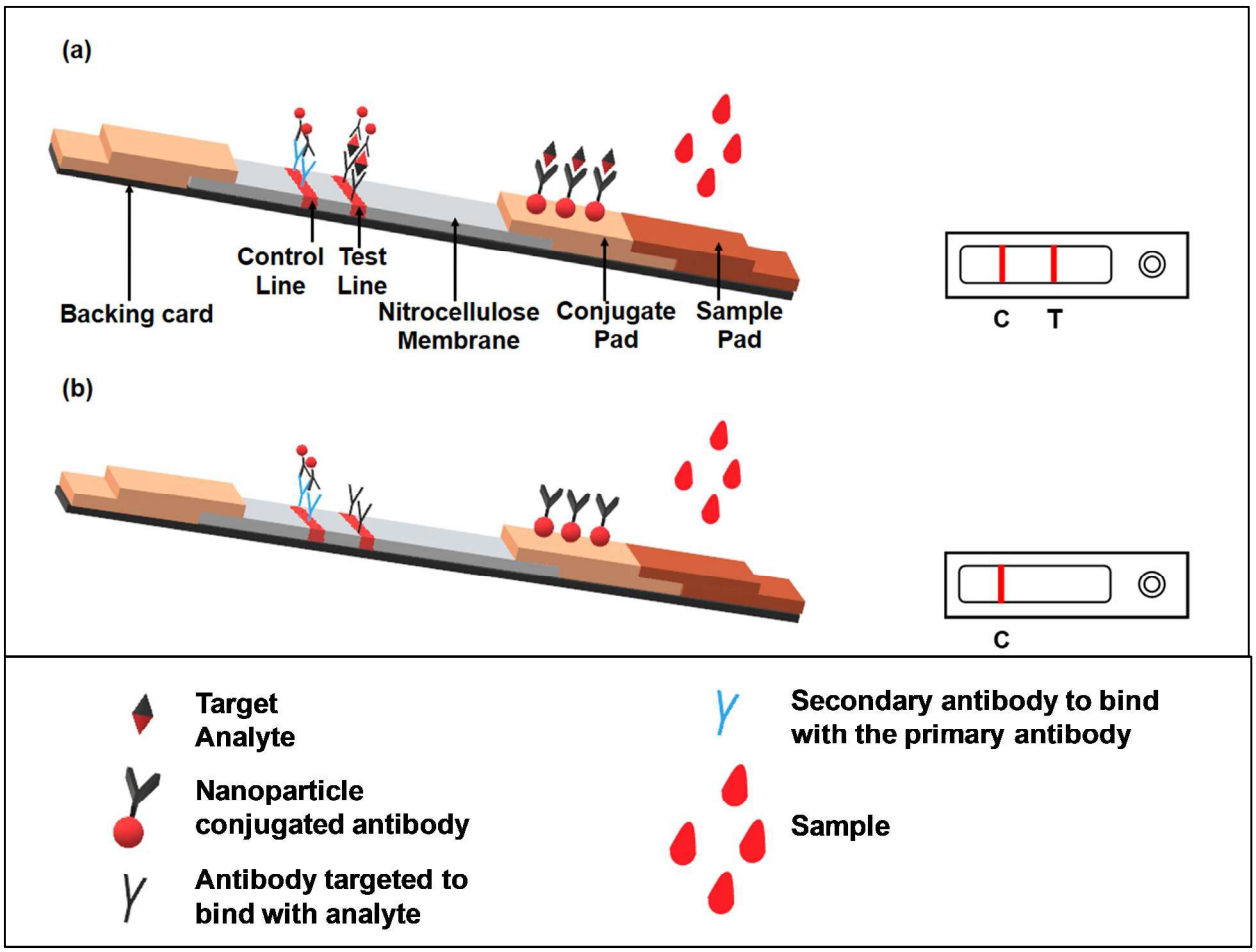

Figure-3: Schematic representation of a LFIA device (a) Positive result while analyte of interest present in the sample, (b) Negative result while analyte of interest is not present in the sample

As shown in the Fig-3; a sample pad, which is placed at one end of the strip helps to promote and evenly distribute the sample to its next component, the conjugate pad. The sample pad is generally made up of cellulose, cross-linked silica or glass fibres [15, 26]. The choice of material to produce sample pad is based on the material's property to hold certain buffer solutions, proteins, surfactants, etc. while applying the test material to facilitate the flow upon addition of buffer [28]. The conjugate pad which is generally made of cross-linked silica is used to hold probe particles and it keeps them functionally stable and active. Additionally, the interaction between the nanoparticles and the sample pad should be weak in order to release the conjugated particle while encountering a moving fluid. This is accomplished by using buffer or mixture of buffers which typically contains carbohydrate molecules. These sugar molecules (like sucrose) stabilize

View Article Online
DOI: 10.1039/C8AN00307F

the probe particles by forming a layer around them thus making the particles shielded from degradation [29]. The probe particles are conjugated to an antibody or a molecule which specifically binds to the target analyte. In most of the cases the probe used is a conjugated colloidal gold nanoparticle (AuNP). However, few recent reports have also demonstrated the used of other nanoparticles like silver [30], carbon [31], selenium [32] or coloured latex particles [33], etc as probe for LFIA devices. After crossing the conjugate pad, the flowing fluid, now also carrying the probe particles which are either free or bound to the target analyte (if present in the sample) comes into a membrane typically made of nitrocellulose. This membrane has two different zones or lines namely Test and Control zones or lines. Biological components mainly antigens or antibodies are immobilised to form these lines. The next step is the interaction between target analyte and specific antibody coated in the Test and Control zones. The design of the assay is made in such a way that if the analyte of interest is present in the sample, it will be captured by the antibody present in the Test zone. This antigen-antibody aggregation will result in developing a colour or band formation at the site of the Test zone depending upon the type of label used (such as AuNPs) [34]. To conclude that the flow through the membrane has been properly established, response in Control zone is observed. It is independent of the target analyte and it will always form the band even if there are no analyte molecules present in the given sample. This happens because of the interaction of the unloaded probe and the antibodies present in the Control zone. A positive test is indicated by the development of bands at both the Test and the Control region, while band formation only in the control zone demonstrates a negative test (Fig-3). Response either only in Test zone but not in Control zone or no response at all in any of the zones is indicative of an invalid result [21].

There are two types of format exploited for the immunoassay- Sandwich and Competitive assay [18]. Sandwich format is applicable for analytes with more than one epitopes. In this case, one site of the target analyte binds with antibody conjugated with label molecule for *eg.* AuNP. This antibody-gold conjugated target analyte then flows through the membrane and it comes into contact with another antibody specific to any other binding site of the target analyte in the Test zone. The capture of antibody-AuNP-antigen conjugate and antibody present in the Test zone makes the pattern or line that can be visually verified or can be detected via optical/magnetic detectors based on the type of label used.

View Article Online
DOI: 10.1039/C8AN00307F

When the analyte is of low molecular weight and/or is a hapten i.e. it has only one binding site or epitope, the competitive format is used. In this format, the signal is negatively correlated with the to the concentration of the analyte [35]. Immobilised analyte conjugated with antibody-AuNP complex is sprayed over the test line giving a strong response in signal. While the analyte flows through the strip, it competitively binds with the antibody and thus releases the antibody-gold nanoparticle conjugate from the Test line and thus the signal gets reduced with increasing concentration of the analyte.

Nanoparticles are widely used as label or probe molecules for detection in LFIA devices. Coloured or fluorescent nanoparticles in the range of 15 – 800 nm is ideal as the small size does not interfere with the flow or the path of the flow. As mentioned earlier, though AuNP is the popular choice for label, there are other nanoparticles that are also been employed. Liposomes incorporated with bioluminescent dyes [36], quantum dots [37], upconverting phosphorus technology [38], Surface Enhanced Raman Spectroscopy (SERS) reporters [39-43] are some of the new approaches for better sensitivity and quantitative analysis.

Surface functionalization is a key part for using nanoparticles as label in LFIA systems. The major role of nanoparticles involving in sensing of specific analytes in LFIA platform is its ability to bind with biomolecules such as antibodies. This conjugation is achieved by adsorption of the ligand moiety to the surface of the nanoparticle. Though weak interaction forces are involved in conjugation process, this can degrade the antibody or the protein attached to it [44]. Hence, surface functionalization of nanoparticles is done prior to conjugation for stability of the conjugated system. Poly(ethylene glycol) (PEG) is the most commonly used polymer to coat the surface of nanoparticles. PEG modified with thiol group (-SH) in one end and carboxy group (-COOH) or amine group ($-NH_2$) in another end is predominantly used as it can attach with the AuNPs surface via thiol bridge and the antibody can attach at the other end via aldehyde-carboxyl/amine interaction [44]. Surface modification with carbohydrate molecules can also be done for potential biosensor and diagnosis application [45]. For a detailed overview on surface functionalization of different nanoparticles, readers may refer to reference 46-49, which is beyond the scope of the present review [46-49].

Another form of LFIA is nucleic acid lateral flow immuno assay (NALFIA), which is used to detect presence or absence of amplified ds-nucleic acid structure (amplicons) specific to the

View Article Online
DOI: 10.1039/C8AN00307F

pathogenic organism. There are several formats reported for NALFIA: 1) ds-amplicon marked with two different tags at two strands; one is biotin labelled and other one is a fluorescent tag. Avidin coated nanoparticle binds to the biotin labelled strand and anti-tag antibody captures the other strand labelled with tag and thus signal produced is directly proportion to the amount of ds-amplicon present [50]. 2) Nanoparticle conjugated reporter probe and biotin tagged capture probe for ss-amplicon detection. The capture probe is immobilised by avidin interaction and the amplicon binds with both the probe to generate the signal [51]. The capture probe can also be BSA tagged or can be simply immobilised in the strip through passive adsorption.

3. LFIA Application strategies for diagnosing infectious disease:

In the following sections we have divided the LFIA devices in two broad categories based on the type of the disease 1. Pathogenic bacterial strains and toxins and 2. Protozoal and viral infection. AuNP is the most exploited nanoparticle reporter in the LFIA devices for its stability, ease-of-synthesis, surface modification and functionalization for desired change in the physical and chemical properties which leads to its optimum function as a reporter molecule as needed for the device. Besides AuNPs, Carbon nanoparticles (CNPs), Quantum Dots (QDs), Up-converting phosphor (UCP) and other nanomaterials are also being used for detection of infectious agents through LFIA. A brief discussion on all the above categories is represented in Table 1 and 2 with focus on reported works with promising results along with some enhancement or modification over the existing techniques for improved sensitivity and detection limits.

Table-1: LFIA devices for detecting Bacterial infection

Bacterial Analyte	Sample used for detection	Type of label	LFIA principle	Sensitivity or LOD	References
Escherichia coli O157	Fecal samples from bovine and swine, raw beef, pork	AuNPs	40 nm AuNP conjugated Murine monoclonal antibody (mAb) to *E. coli* O157:H7 lipopolysaccharide (LPS)	1.8×10^5 CFU/mL without enrichment and 1.8 CFU/mL after enrichment Specificity: pork (98.8%), bovine feces (87.9%) and swine feces (93.4%)	[52]
Escherichia coli O157:H7	milk powder, flour, starch, coffee, biscuit, cake, jelly and juice.	AuNPs	Colloidal gold conjugated double antibody sandwich assay	1×10^5 CFU/mL with no cross-reaction with 30 strains of 24 species in Enterobacteriaceae (including non-O157 *E. coli, Salmonella, Shigella, Proteus, Citrobacter, Enterobacter, Serratia* and *Yersinia), Staphylococus, Listeria, Aeromonas* and *Vibrios*	[53]
	Spiked milk, purified water and beef	AuNPs	Colloidal gold conjugated with *E. coli* O157:H7 mAbs. Immunomagnetic separation (IMS) is done by immunomagnetic particle (IMP) conjugated	Without IMP 10^5 CFU/ml With IMP 10^3 CFU/ml Sensitivity: 95.5%	[54]

			with *E. coli* O157:H7 polyclonal antibodies (pAb)		
Escherichia coli O157:H7	Culture both	Fluorescent microsphere	Fluorescein isothiocyanate fluorescent microspheres conjugated with *E. coli* O157:H7 mAbs.	1.6×10^3 CFU/mL	[55]
Escherichia coli O157 *Salmonella typhimurium*	Culture broth	AuNPs	AuNP conjugated with antibodies against *E. coli* O157 and *S. typhimurium*	*E. coli* O157: 10^5 CFU/mL *S. typhimurium*: 10^6 CFU/mL	[56]
Escherichia coli	Standard buffer, bottled water and milk samples	Streptavidin-QD 655 (quenching by Graphene oxide (GO) in absence of pathogen (OFF state))	Streptavidin-QD conjugated biotinylated antibody against *E. coli* followed by treatment with GO	10 CFU/mL in standard buffer 100 CFU/mL in bottled water and milk	[57]
Salmonella enteritidis	Raw eggs	AuNPs	anti-*S. enteritidis* antibodies conjugated to colloidal gold particles	10^7 CFU/mL No cross reactivity with *Salmonella typhimurium*	[58]
	Bacteria spiked milk powder	AuNPs	15nm AuNP conjugated DNA	10 CFU/mL	[59]
		AuNPs	AuNPs conjugated 16s rDNA/rRNA	5 fmol for synthetic DNA	[60]
Staphylococcal Enterotoxin B	Simulated samples of human urine, serum and cow milk	AuNPs	25 nm AuNP conjugated with purified anti-SEB IgG	1 ng/mL With silver enrichment: 10 pg/mL	[61]

	powder				
Anthrax (*Bacillus anthrax*)	Milk, water samples	AuNPs	IMS of anthrax spores followed by lateral flow assay with AuNP as label	5×10^5 CFU/mL	62
Bacillus anthracis	Culture media	super-paramagnetic nanoparticles	mAb 12F6 conjugated to super-paramagnetic iron oxide particles	400 pure *B. anthracis* spores $4{\times}10^3$–10^6 CFU mL^{-1}	63
Bacillus anthracis	Spiked samples of milk powder, starch and baking soda	Carboxylated super-paramagnetic iron oxide particles	mAbs 12F6 against *B. anthracis* conjugated with super-paramagnetic iron oxide particles	500–700 pure *B. anthracis* spores $6{\times}10^4$ spores/g in milk powder, $2{\times}10^5$ spores/g in starch and $5{\times}10^5$ spores/g in baking soda	64
Enteropathogenic *E. coli* (EPEC) and Enterohemorrhagic *E. coli* (EHEC)	Supplemented stool sample	AuNPs	AuNP conjugated anti-EspB IgG	4 ng/mL In stool sample: 0.06 μg/mL Sensitivity: 96.9%	65
Campylobacter jejuni	Fecal extract	AuNPs	mAb (4B4) against a 15KDa cell surface antigen-colloidal gold conjugate	1.8×10^4 to 8.2×10^4 CFU/mL Sensitivity- 84.8%	66
Aflatoxin B1 (AFB1)	Culture media	GO or carboxylated GO (GO-COOH)	Anti-AFB1 mAb labeled with GO or GO-COOH	Visual LOD: 0.3 ng/mL	67
Aflatoxin B_2 (AFB_2)	Culture media	Magnetic nanogold microspheres with	Monoclonal anti-AFB2 antibody (clone 3A7)	27 μg/kg	68

		nano-Fe_2O_3 particles as core and AuNPs as shell	conjugated Nano-Fe_2O_3 particles		
Aflatoxin M1 (AFM1)	Spiked raw milk	Immuno magnetic nanobeads (MNB)	MNBs conjugated with anti-AFM1 antibody	0.1 ng/ml in raw milk	[69]
Aflatoxin M1 (AFM1)	Raw milk samples	Immuno MNB	Anti-AFM1 mAb conjugated MNBs	0.02 µg/L	[70]
Fumonisin mycotoxins	Maize flour sample	CdSe/ZnS QDs	BSA tagged fumonisin antigen conjugated with QD (fluorescence quenching by AuNP conjugated anti-fumonisin antibody)	Visual LOD: 1.56–6.25 ng/ml	[71]
Botulinum (*Clostridium botulinum*)	Spiked fecal sample	AuNPs	AuNP conjugated monoclonal Botulinum Neurotoxin Type D (BoNT/D) antibody	50 pg/ml	[72]
	Spiked samples of serum, urine and cooked meat broth	AuNPs	AuNP conjugated anti-BoNT/A heavy chain mAb (44.1)	50 ng/ml With silver enhancement: 1 ng/ml	[73]
	Spiked milk sample, orange and apple juice	AuNPs	AuNP conjugated with two different mAbs: F1-51 (BoNT/A HC-specific) and BoB-92-32 (BoNT/B HC-specific)	In 2% and 1% milk BoNT/A: 5 ng/ml BoNT/B: 10 ng/ml In diluted apple juice BoNT/A: 25 ng/ml BoNT/B: 10 ng/ml	[74]

				No cross reactivity between BoNT/A and BoNT/B	
Staphylococcus aureus	Pork, raw chicken, crab meat and inoculated beef, fried chicken, corn flake, cooked rice, noodle	AuNPs	anti-protein A IgG was conjugated with AuNPs	Sensitivity: 100% with 28 *S. aureus* strains and 23 non-*S. aureus* strains	[75]
	Naturally contaminated food samples	AuNPs	anti-protein A IgG conjugated AuNP	Sensitivity:100% Specificity: 96-100% with 44 non-*S. aureus* strains	[76]
	Respiratory samples	AuNPs	Monoclonal anti-*S. aureus* antibody conjugated 40 nm colloidal gold particles	10^6 CFU/ml	[77]
Staphylococcus enterotoxin B (SEB)	Spiked tap and surface water, apple juice, raw milk, ham extracts, cheese extracts	Sulforhodamine B (SRB)-encapsulating immunoliposomes	Dextran/BSA/rhodamine B isothiocyanate conjugated thiol derivatized anti-SEB antibody.	20 pg/ml (Liner range: 0.02-5 ng/ml)	[78]
	Recombinant SEB	Hollow gold nanospheres (HGNs) with Malachite green isothiocyanate (MGITC) as Raman reporter (Raman-active probe)	Anti SEB pAb	0.001 ng/ml	[40]

Stretococcus suis	Bacteria isolated from diseased piglets, healthy piglets and human patients	AuNPs	AuNP conjugated antibody against SS2 (serotype-2)	10^6 CFU/ml	[79]
	Bacterial culture solution	AuNPs	colloidal gold coated with pAbs against serotype 2 capsular polysaccharides (CPS)	10^4 CFU/ml 0.05 µg of CPS	[80]
Pneumolysin (*Streptococcus pneumoniae)*	Pneumolysin sample	Au@Ag with Rhodamine as SERS reporter	Au@Ag with Rhodamine as SERS reporter conjugated anti pneumolysin antibody, PLY-7)	1 pg/mL	[41]
Enterobacter cloacae	Simulated water sample	AuNPs	colloidal AuNPs conjugated with monoclonal anti-*E. cloacae* antibody	10^2 CFU/ml	[81]
Enterobacter sakazakii	Spiked infant formulae samples	CNP	Neutravidin labelled CNP to bind with biotin tagged amplicon	<10 cells of *Cronobacter* sp. per 10 g	[82]
Leptospira sp.	Human sera	AuNPs	Leptospira specific antibody against broadly reactive leptospiral antigen and colloidal gold-labelled anti-human	Sensitivity: 85.8% Specificity: 93.6%	[83]

			IgM antibody		
	Culture media	AuNPs	colloidal AuNPs conjugated mouse anti-fluorescein antibody to detect m-LAMP label based biotin/fluorescein labelled *LipL32* gene amplicons	Specificity: 100% LOD: DNA concentration 3.95×10^{-1} genomic equivalent ml^{-1}	[84]
Vibrio cholerae Serogroup O1 and O139	Culture media	AuNPs	Murine mAb against V. cholerae LPS conjugated AuNPs	Sensitivity: 93-100% (O1), 100% (O139) Specificity:100% (O1), 98-100% (O139) 10^8 and 10^7 CFU/ml for O1 and O139 respectively.	[85]
Vibrio cholerae O139	Seafood samples	AuNPs	VC-273 Mab conjugated to AuNPs	10^4 CFU/ml 1 CFU/ml with pre-incubation of sample with in alkaline peptone water for 12 hours	[86]
Vibrio parahaemolyticus	Culture media grown bacterial antigen	CdTe QDs	pAb against *V. parahaemolyticus* conjugated with CdTe QDs; quenching by mAb	5.03×10^4 cfu/L	[87]

			labelled AuNPs		
Treponema pallidum (Syphilis)	Serum samples from 8 geographically diverse sites	AuNPs	9 commercially available rapid Syphilis tests	Sensitivity: 84.5-97.7% Selectivity: 84.5-98%	88
Mycobacterium tuberculosis Tuberculosis (TB)	Whole blood and serum spiked with *M. tuberculosis* antigen	AuNPs	40 nm AuNP conjugated with protein-A	5 ng/ml	89
Listeria monocytogenes	Bacterial culture	AuNPs	AuNP conjugated nucleotides to detect hlyA mRNA	0.5 pg/μl of genomic RNA 20 CFU/ml	90
Listeria monocytogenes	Spiked milk samples and other food samples (including salad, frozen vegetables etc.)	CNP	CNP-neutravidin conjugate to bind to biotin modified aptamer	0.1 ng of labelled amplicon 50 pg of *L. monocytogenes* template DNA (approximately 10^5 cells)	91
Helicobacter pylori	Human fecal sample	AuNPs	mixture of DF2a and IH10b mAb conjugated AuNP	10^4 CFU/mL	92
Cronobacter spp.	Pure culture and powdered infant formula (PIF)	AuNPs	Biotin labelled 16s ribosomal DNA of *Cronobacter* sp. detected using streptavidin linked AuNPs	10^7 CFU/mL	93
Salmonella typhimurium	Bacterial culture derived antigen	Liposome entrapped Methylene Blue (MB)	Thiol derivative of anti-*Salmonella* antibody	1,680 cells	94

			conjugated with maleimide-derivatized liposomes containing MB		
Salmonella choleraesuis	Pure culture and spiked whole milk samples	Gold magnetic bifunctional nanobeads (GMBN)	anti-*S. choleraesuis* mAbs (11D8-D4) conjugated GMBN	Sensitivity:5 × 10^5 CFU/mL	[95]
Brucella sp	Bacterial culture	UCP	pAb against *B. melitensis* M55009 covalently coupled with UCP particles	2.0 × 10^3 to 3.9 × 10^5 CFU/mg	[96]
Pantoea stewartii subsp. *stewartii*	Spiked corn seed samples	Lanthanide (Europium chelate-coated silica nanoparticles)	Anti-Pss antibody conjugated Europium chelate-coated silica nanoparticles	10^4 CFU/mL	[97]
Y. pestis and *B. pseudomallei*	Bacterial culture	UCP	mAb against *Y. pestis* and *B. pseudomallei* conjugated UCP	Sensitivity: 10^3 CFU/test	[98]
Pseudomonas aeruginosa and *Staphylococcus aureus*	Bacterial Culture	AuNPs	AuNP conjugated pAb against *P. aeruginosa* and *S. aureus*	500-5000 CFU/mL Specificity: 100%	[99]
E. coli O157:H7 and *Salmonella typhimurium*	Recovered bacteria from contaminated lettuce	AuNP	AuNP conjugated anti-S. aureus and anti-E. coli O157 antibody	*E. coli* O157:H7: 1.87 × 104 CFU *S. typhimurium*: 1.47 × 104 CFU After enrichment *E. coli* O157:H7: 1 CFU	[100]

				S. typhimurium: 1 CFU	

View Article Online
DOI: 10.1039/C8AN00307F

3.1. LFIA for detecting bacteria and bacterial infections

There are various bacterial toxins and food borne infectious diseases where LFIA devices are used for rapid detection. Staphylococcal enterotoxin B (SEB) has been reported to be detected using 25 nm colloidal gold as label with anti-SEB IgG with detection limit of 1 ng/mL in less than 5 minutes [61]. An improvement over conventional SEB detection was reported by using fluorescent immunoliposomes which allowed the detection of SEB close to 20 pg/mL [78]. SERS based enhancement for detection of SEB has shown detection limit of 0.001 ng/mL. Here, MGITC, a SERS reporter conjugated with gold nanospheres has been used as label in the assay [40]. Anthrax, a deadly infectious disease caused by *Bacillus anthrax* has also been investigated through LFIA. Anthrax incidents in 2001 and its potential to be used as a weapon in bioterrorism led researchers to develop method for fast and sensitive detection of spores causing anthrax in food and feeds [101, 102]. For this, an additional step of IMS was performed prior to subjecting the sample to a LFIA device. This has proved successful in sensing spores of *Bacillus*

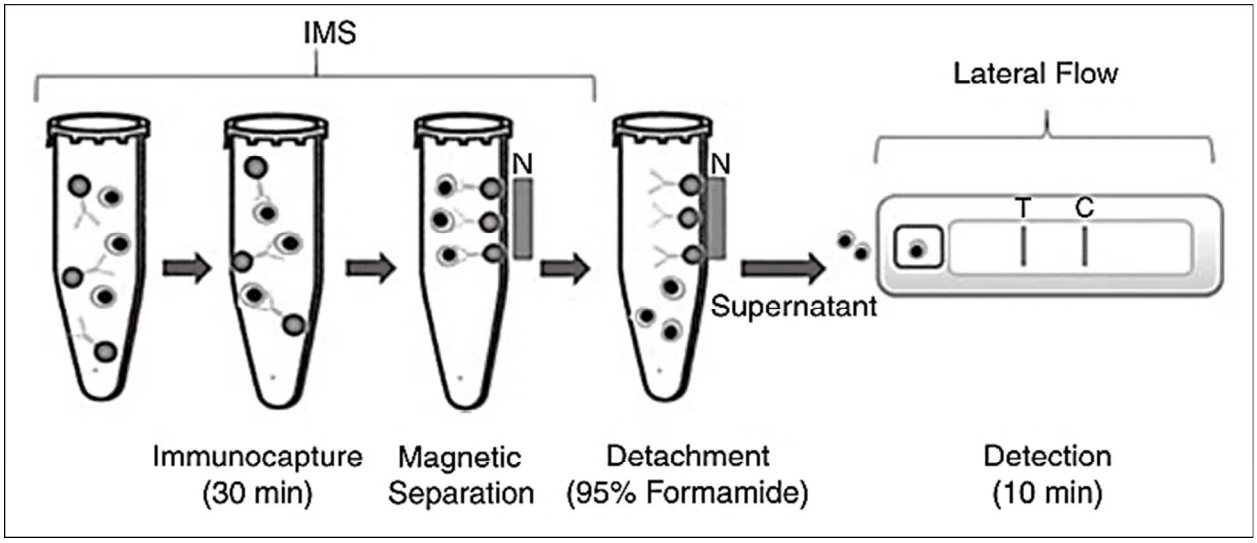

Figure-4: Principle of IMS and LFIA for detection of *Bacillus anthrax* spores. Anti-spore antibodies coupled with COOH-magnetic beads are used for immunocapture. Magnetic separation is achieved by using magnetic field. The spores are recovered using Formamide and EDTA and are used directly in LFIA device. Reprinted (adapted) with permission from [62]. Copyright (2009) John Wiley and Sons.

View Article Online
DOI: 10.1039/C8AN00307F

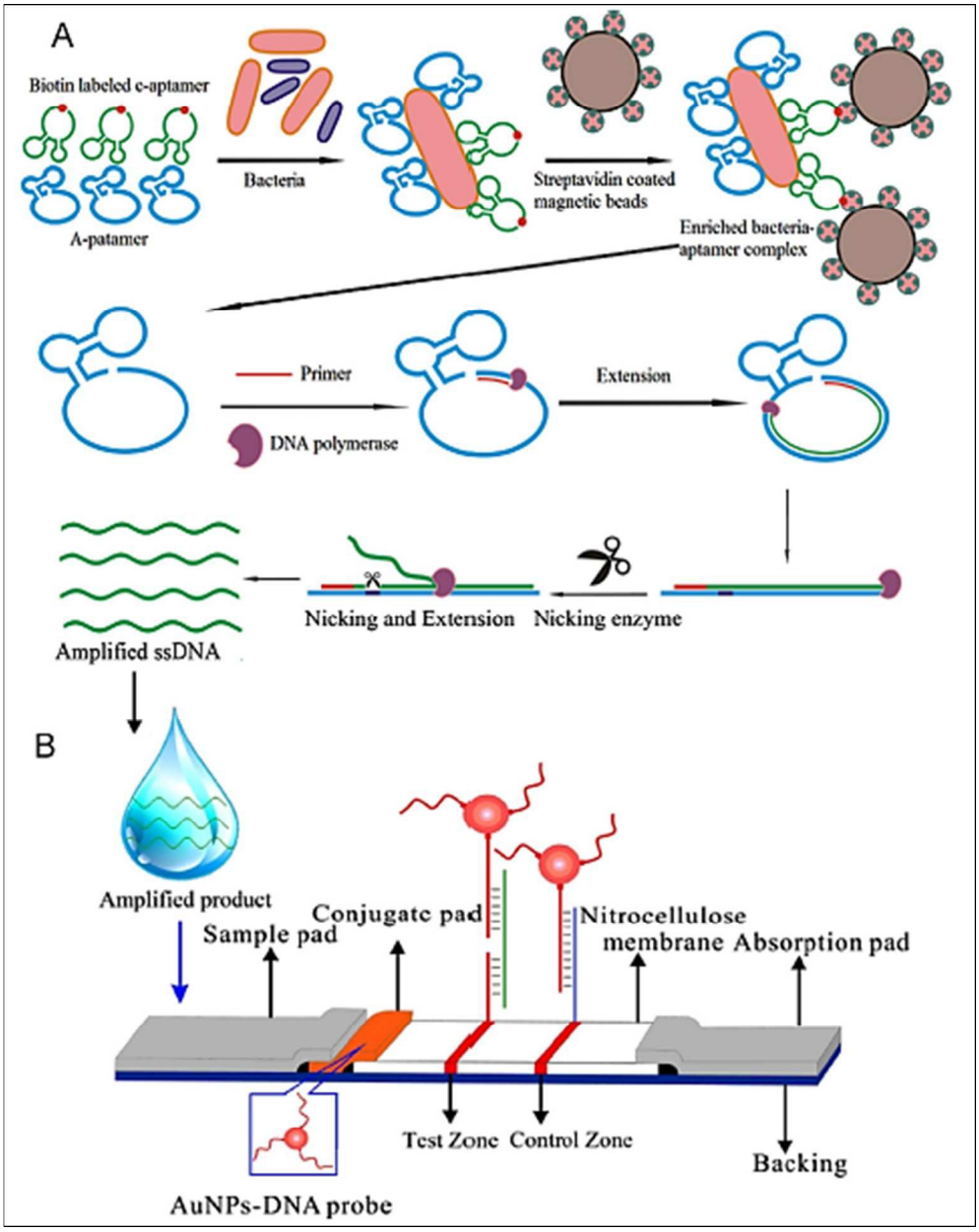

Figure-5: Schematic design of aptamer based detection of *Salmonella enteritidis*, A. Magnetic separation using streptavidin coated magnetic bead. The biotin labelled aptamer bound bacteria is detected by streptavidin interaction and magnetically separated which is followed by strand displacement amplification leading to production of amplified sample containing ss DNA, B. The LFIA strip containing ss DNA-AuNP probe for detection. Reprinted (adapted) with permission from [59] Copyright (2014) Elsevier.

View Article Online
DOI: 10.1039/C8AN00307F

anthracis in water and dairy products with a spore recovery of 95% from IMS [62] with 10^5-10^7 CFU mL^{-1} of spores in milk or water sample. IMS is achieved by using anti spore antibodies conjugated with COOH-magnetic beads. Magnet is used to separate the complex and formamide and EDTA are used to elute the spores which are then used in the LFIA device (Fig-4).

Human salmonellosis diagnosis had also been established by LFIA which was designed to detect *Salmonella enteritidis* with a detection limit of 10^7 CFU/mL without any cross reactivity with *Salmonella typhimurium* [58]. As low as 10 CFU/mL of *Salmonella enteritidis* was detected by using aptamer based strand displacement amplification (SDA) [59]. In this process, the bacteria are first mixed with excess amount of aptamers of two types which specifically binds to the bacteria. One of which is biotin labelled and the other carries the sequence for SDA. Then streptavidin labelled magnetic beads are used for magnetically separating the *S. enteritidis* bacterium from other species. This magnetic bead- aptamer-bacteria complexes are then directly amplified by SDA and the amplified product containing ssDNA is applied on LFIA test strip and subsequently detected as shown in Fig-5. A Gram negative bacterial strain, *Escherichia coli* O157:H7 causes hemorrhagic colitis and hemolytic uremic syndrome in humans [103]. LFIA strip for rapid detection of *E. coli* O157:H7 was developed by Jung *et. al* in 2005. This assay is based on murine mAb to the said antigen (*E. coli* O157:H7 LPS) conjugated with 40 nm colloidal AuNPs with a lowest detection limit of 1.8×10^5 CFU/mL without any enrichment [52]. Later study has reproduced similar detection limit viz. 1×10^5 CFU/mL from various food samples *viz.* milk powder, flour *etc.* [53]. Immunomagnetic enrichment technique has further increased the sensitivity for the detection of *E. coli* O157:H7 with detection limit of 10^3 CFU/mL with 95.5% sensitivity and 100% specificity [54]. Another study has reported aptamer mediated magnetic enrichment as well as strand displacement amplification method for the detection of *E. coli* 0157:H7 with a detection limit of 10 CFU mL^{-1} [104]. In this study, they had used two different aptamers which selectively binds to two different outer membrane proteins of *E. coli*. One of the aptamers were biotin labelled which were magnetically enriched by streptavidin labelled magnetic beads separation. The other aptamer was used for amplification and subsequently targeted for detection via NALFIA. In this context, carbon-based nanoparticles and nanomaterials are also been exploited as label in LFIA devices. Carbon based nanoparticles was preferred for their very low production cost, high contrast signal and ease of scaling-up reactions [19]. Fluorescence quenching

View Article Online
DOI: 10.1039/C8AN00307F

of QDs by GO 2D nanosheets as mechanism of detection has been used to detect as low as 100 CFU/mL of *E. coli* in

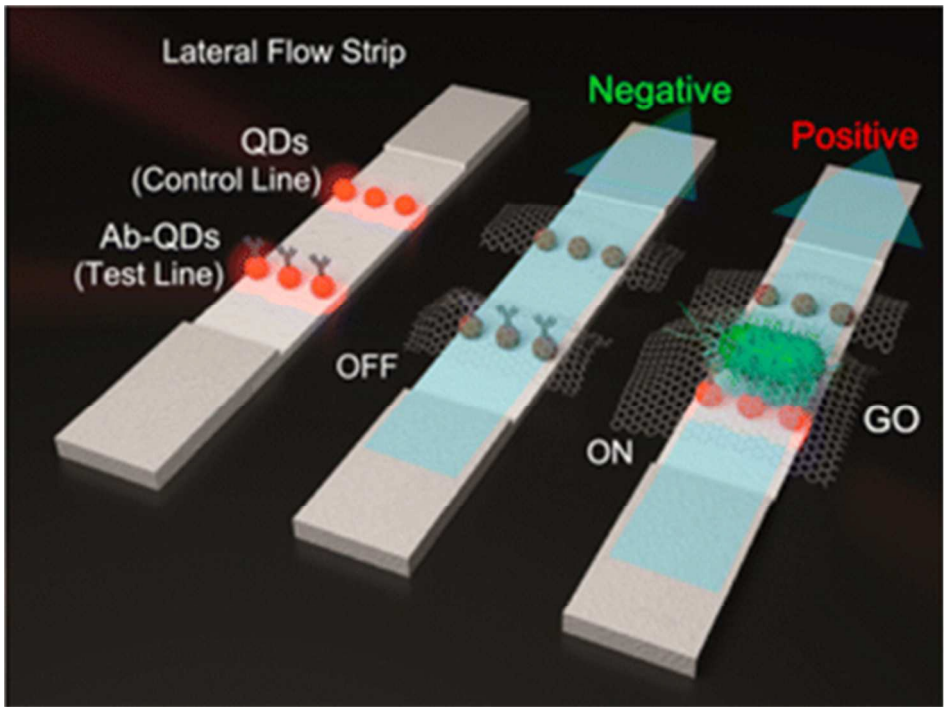

Figure-6: Schematic representation of the working mechanism of GO quenching mechanism of fluorescence in absence (OFF mode) and presence (ON mode) of bacteria. Reprinted (adapted) with permission from [57]. Copyright (2015) American Chemical Society.

bottled water and milk samples [57]. The detection mechanism is described in Fig-6. When the analyte is not present in the sample GO can effectively quench the fluorescence of the QDs (OFF mode). In presence of analyte, this quenching is hindered and fluorescence signal is detected (ON mode). Detection of EPEC and EHEC by using AuNP based LFIA are also reported with a specificity and sensitivity of 100% and 96.9% respectively [65]. In-solution hybridization for detection of specific sequences of 16S ribosomal RNA has allowed to detect 5×10^4 CFU/mL of *E. coli* within 25 minutes (Fig-7) [105]. *Campylobacter* species are reported as the causative agent for human bacterial gastroenteritis in many industrialized countries [106]. A 15 KDa cell surface protein of *Campylobacter jejuni* has been targeted for the rapid detection by LFIA from human fecal extract. Within 15 minutes, a specificity of 100% and a sensitivity of 84.8% was achieved with the designed LFIA device [66].

View Article Online
DOI: 10.1039/C8AN00307F

There are various enterobacteriaceae family members (like *Shigella* sp., *Aeromonas* sp. etc.), detection of which can be carried out by LFIA devices. The detailed description about these LFIA

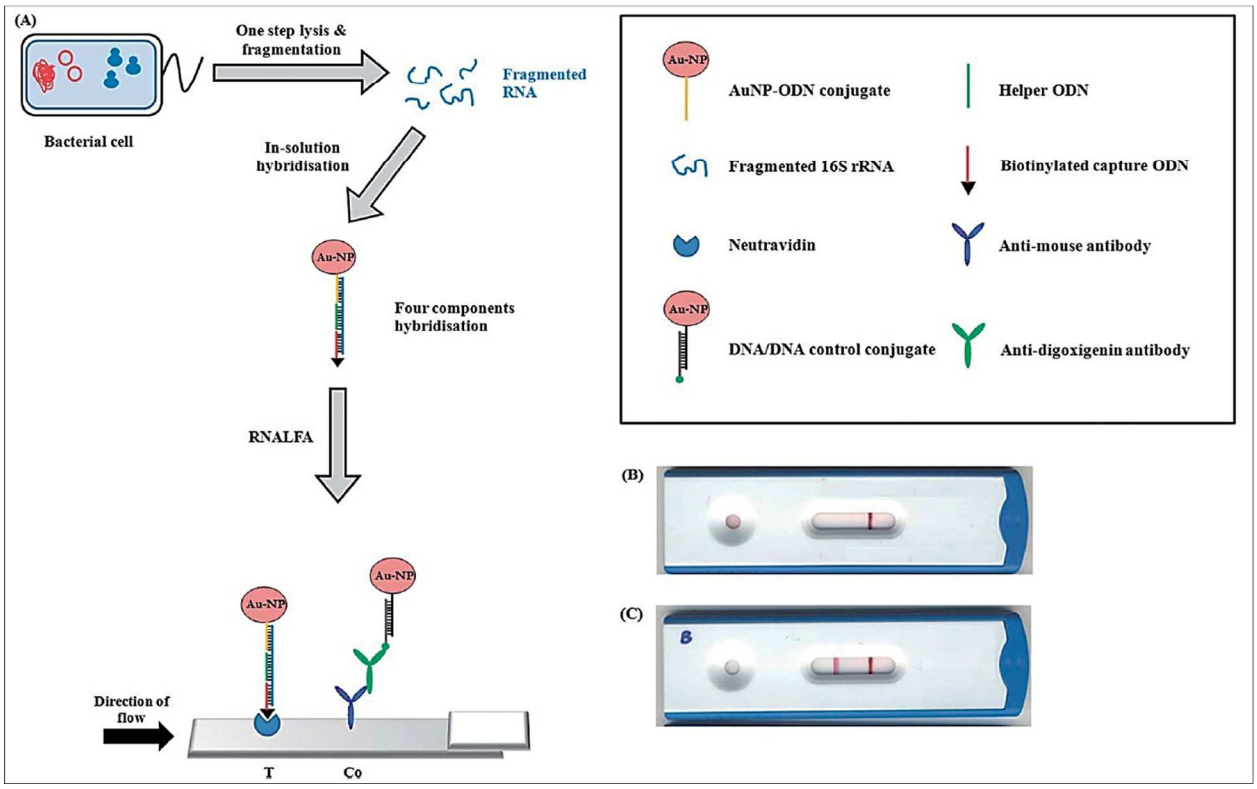

Figure-7: Principle of Ribonucleicacid Lateral Flow Assay (RNALFIA); A. Lysis and subsequent fragmentation of E. coli cells produces fragmented RNA which is required for the Four component hybridization with AuNP-oligodinucleotide (ODN) conjugate, Biotinylated capture ODN and a Helper ODN. This hybridized assembly is then applied on the lateral flow strip with Neutravidin immobilized at Test line and anti-mouse antibody at Control line. Reprinted (adapted) with permission from [105]. Copyright (2014) Royal Society of Chemistry.

device can be found in [107]. Enterobacteriaceae family members are known for causing various water borne diseases. They produce various endotoxins and exotoxins which causes the pathogenesis of the infection by interacting with the digestive juices resulting in enormous water loss from the body. Botulism is a fatal infectious disease caused by a neurotoxin botulinum (BoNT) produced by *Clostridium botulinum* and is capable of causing paralytic illness in human when found even in very small amount in food [108]. The toxin is classified in 7 antigenic types (A-

View Article Online
DOI: 10.1039/C8AN00307F

G) based on their absence of cross-neutralization e.g. anti-G antitoxin does not neutralize toxin type A-F [109]. Detection of BoNT/D by sandwich format LFIA has been established using AuNPs as label with a detection limit of 50 pg/mL [72]. Similar strategy has been used for BoNT/A detection where mAb against BoNT/A conjugated with AuNP has been used. This detection showed no cross reactivity with BoNT/B or BoNT/E when silver enhancement reagent was used to amplify the signal generated from colloidal gold. The detection limit for this LFIA strip was found to be 1 ng/mL [73]. Simultaneous detection of BoNT/A and BoNT/B is reported by using separate mAbs with high affinity and specificity for the two mentioned serotypes [74]. Another bacterium, *Staphylococcus aureus* is the leading cause of food poisoning specially in processed and canned foods [110]. LFIA based on sandwich format was developed for detecting *S. aureus* in processed food (pork, beef, fried chicken) [75]. The sensitivity of the immunochromatography test was found to be 100 % when tested with 28 *S. aureus* and 23 non-*S. aureus* strains. *Stretococcus suis* has been identified as a causative agent of meningitis, endocarditis in humans [111, 112]. A LFIA strip based on colloidal AuNPs has been developed against serotype 2 which is the most common and pathogenic both to humans and pigs [79]. The sensitivity of the immunochromatography strip was found to be 10^6 CFU/mL. A recent breakthrough in detecting *Enterobacter cloacae* was achieved by using IMS of *E. cloacae* from sample and then detecting it with monoclonal anti-*E. cloacae* antibody conjugated with colloidal AuNPs [81]. *E. cloacae* can induce various pathogenic conditions including respiratory tract infection, urinary system infection, skin and soft tissue infection, and septicemia [113, 114]. The LFIA test strip showed 10^2 CFU/mL of *E. cloacae* detection with IMS which is 10 times lower LOD than that of the direct detection. mAb against *Vibrio cholerae* subtype O1 and O139 has been used with colloidal gold for multiplexed detection of the subtypes of *V. cholerae*. The detection limit of the device was found to be 10^8–10^7 CFU/mL [85]. There are several toxins (like mycotoxins, aflatoxins etc.) produced by various bacteria or fungi, some specific type of bacterial infection (like Listeria sp. infection) are extensively described in other reviews [23, 115-119].

Table-2: Comparative study on various viral and protozoal diseases in regards with LFIA based diagnosis

				LFIA Based Diagnosis				
Disease Condition	**Causing agent**	**Laboratory diagnosis**	**Sensitivity or LOD/Drawback**	**Type of label**	**Analyte**	**Label used**	**Sensitivity or LOD**	**References**
Protozoal								
1. Malaria	Plasmodium falciparum (major) Other Plasmodium species	Laboratory-based thin blood smear microscopy	Parasitemias of 50 parasites/ µL	AuNP	Plasmodium Lactate Dehydrogenase (pLDH)	Colloidal AuNP labelled pan-specific-anti-pLDH-mAbs	Parasitemias of ≥ 100 parasites/µL	[120]
				AuNP, Silver nanoparticle (AgNP)		Ni(II)-nitrilotriacetic acid (NTA) functionalised AuNP and AgNP	2000 parasites/µL parasitemia	[121]

				AuNP		Thermally responsive magnetic nanoparticle (MNP)	10 ng/mL of pfHRP-II	[122]
				AuNP		AuNP conjugated anti-pLDH with QR barcodes linked with Google Analytics	10 ng/mL of recombinant pLDH	[123]
				AuNP		Micellar Aqueous Two-Phase System (ATPS) with anti-pLDH conjugated AuNP	1 ng/ µL	[124]
				CNP	Biotin labelled 18s RNA of *Plasmodium sp*	Neutravidin labelled CNP to bind with biotin tagged amplicon	0.3 to 3 parasites/µL	[31]
Leishmaniasis	*Leishmania*	Skin biopsies, ELISA,	Sensitive but time	AuNP	Leishmania infantum kinetoplast DNA	20 nm AuNP conjugated	0.038 parasites (1 parasite/100	[125]

	infantum	Immunofluorescence	consuming and difficult to operate			pAb to recognize anti-FITC antibodies.	µL of DNA sample)	
Schistosomiasis	*Schistosoma sp.*	Eggs identification in stool, ELISA, Microscopy	Time consuming and highly expertise technician and facilities are must	Up-converting phosphor (UCP)	*Schistosoma* Circulating Anodic Antigen (CAA)	Mouse monoclonal anti-CAA antibody 147 coupled to 400 nm UCP reporter particles	0.5 pg/mL	[126]
	S. haematobium			UCP	*Schistosoma* CAA	Mouse monoclonal anti-CAA antibody 147-3G4 coupled to 400 nm UCP reporter particles	30 pg CAA/mL serum; (equivalent to about 10 worm pairs)	[127]
Viral								
Influenza	Influenza virus with different subtypes	HI assay, seroconversion detection between acute- and	HI Assay: 92%	AuNP	Hemagglutinin (HA)	AuNP labelled Mab against HA	0.25 HA units	[128, 129]

		convalescent-stage samples						
				AuNP	M gene, H1, H3. H5 gene	streptavidin coated AuNPs linked with the biotin moieties incorporated in the middle of the DNA strands	10^2 copies	[130]
				AuNP		AuNPs to capture biotin labelled reverse-transcription loop-mediated isothermal amplification (RT-LAMP)	10 copies	[131]
				AuNP	Flu A antigen, Flu B antigen	Silver growth on AuNP conjugated anti-Flu A	Sensitivity and specificity: Flu A- 91.2% and 95.8 % Flu B-94.4% and 98%; respectively	[132]

				AuNP	Nucleoprotein and matrix protein	Anti-nucleoprotein (NP4) MAb and anti-matrix protein (M1) MAb conjugated AuNP (15 nm)	47 $TCID_{50}$ /mL	[133]
				AuNP	HA	Anti-HA (H3, H5, H7, H9) antibody conjugated AuNP to detect biotin tagged aptamer captured specific virus	2×10^6 virus particles	[134]
				Cy5 doped silica nanoparticles	Influenza A	mAb against influenza A nucleoprotein conjugated Silica nanoparticles	250 ng/mL	[135]
Hepatitis	Hepatitis Virus Type-A,	Liver Biopsy	Time consuming with need of	AuNP	HBsAg, HBeAg	Colloidal Gold labelled antibody	HBsAg- 95% HBeAg- 80%	[136]

	B, C, E (HAV, HBV, HCV, HEV)		skilled technician and well-equipped laboratory			against HBsAg		
				AuNP	HEV IgM	Anti-human-IgM MAb, colloidal gold labelled antibody to HEV preincubated with HEV antigen	93%	[137]
				AuNP	IgM antibody specific to HEV	colloidal gold-labeled anti-HEV mAb 4B2 and recombinant protein EP2.1	96.7%	[138]
				Fluorescent lanthanide	HCV	Eu3+-chelate conjugated recombinant Multiepitope protein (MEP)	Sensitivity: Secondary antibody assay-95.6% Double-antigen assay-91.4%	[139]

				UCP	Hepatitis B surface antigen (HBsAg)	HBsAg conjugated UCP	60 mIU/mL	[140]
				ZnSe/CdSe/CdS/$Cd_xZn_{1-x}S$/ZnS QDs	HBsAg	HBsAg conjugated QDs	0.05 ng/mL	[141]
				Carboxyl modified CdSe/ZnS QDs	HBsAg	anti-HBsAg mAb-labeled QB	75 pg/mL	[142]
AIDS	HIV	HIV ELISA, HIV Viral Load Test, Quantitative PCR	95-100% (~1 ng/mL)	AuNP	HIV-1 p24 antigen	anti-HIV-1 p24 antibody-Selenium colloid based sandwich format with monoclonal biotinylated anti-HIV-1 p24 antibody	25 pg/mL	[143]
				AuNP	HIV-1 p24 antigen	Mouse mAb conjugated to super-paramagnetic particles (200-300 nm)	30 pg/mL	[144]

	AuNP	HIV-1 RNA	AuNP labelled probe (partially complementary strand)	10.5-13 $\log_{10}$ copies/mL (50 copies of *gag* RNA)	[145, 146]
	CNP	p24 antigen	Mouse monoclonal anti-p24 mAb108 coupled to CNP	LOD: 50 pg/mL Sensitivity: 90% Specificity: 100%	[147]
	Platinum core-shell nanocatalyst (PtNC)	p24 antigen	Anti-HIV-1/2 conjugated PtNCs	0.8 pg/mL	[148]
	AuNP	HIV-1 nucleic acid sequence	AuNP conjugated amplification probe and AuNP conjugated complementary and detector probe	0.1 nM	[149]
	Surface modified AuNP by MGITC as Raman reporter (Raman-active	HIV-1 nucleic acid sequence	Raman-active probe conjugated detection DNA	0.24 pg/mL	[150]

				probe)		sequence		
Adenoviral diseases	Adenovirus	Virus isolation from tissue culture	100% (takes 3-4 weeks)	AuNP	Adenovirus capsid hexon (signal antibody)	gold colloid-conjugated mouse mAb to adenovirus capsid hexon	72.6% (within 10 minutes)	[151]
				AuNP	Recombinant HA of H5N1	mAb 25/2 conjugated AuNP	250 ng/ml without amplification 0.5 ng/ml with silver amplification	[152]
				AuNP (later dissolved, collected and GSH capped CdTe QDs added for fluorescent detection)	Avian Influenza Virus (AIV)	AuNP conjugated AIV mAb	0.09 ng/ml Sensitivity: 100% Specificity: 88.2%	[153]
WNV infection (mostly asymptomatic)	Western Nile Virus (*Flaviviridae* family)	WNV IgM/IgG Capture (MAC) ELISA	100% (takes 2-3 days)	AuNP	WNV antigen (protein E)	Colloidal gold particles conjugated Flavivirus specific mAb (6B6C-1)	95-100% agreement with results from CDC WNV IgM/IgG ELISA (within 15	[154, 155]

							minutes)	
Dengue	Dengue Virus (DENV)	Virus Isolation, ELISA, RT-PCR	1-10 infectious virus particles, 1-100 PFU/ml (PCR) (takes days to weeks)	AuNP	NS1 dengue antigen, Anti-dengue IgM and IgG	colloidal gold-labelled specific mAbs against dengue NS1 antigen, IgM, IgG, or IgA	90-100%	[156-163]
				AuNP	Dengue specific IgG	Streptavidin conjugated 40 nm AuNPs	---	[164]
Chikungunya	Chikungunya virus (CHIKV)	Virus Isolation, RT-PCR	Relative sensitivity 100% with PCR	AuNP	Chikungunya Envelope Proteins (E1, E2, E3), CHIKV specific IgM	Colloidal gold-conjugated anti-IgM antibody against CHIKV specific IgM and CHIKV recombinant envelope protein in test line	90-100% (arguable as per multiple studies)	[165-169]

Herpes Simplex Virus (HSV) infection	HSV-2	Virus Isolation, RT-PCR, ELISA	Relative sensitivity 95-100% with ELISA	AuNP	HSV-2 specific IgG	Colloidal gold-conjugated anti IgG antibody with gG1 and gG2 in pre-absorption line and Test line respectively	Sensitivity: 100% Specificity: 97.3 %	170
Newcastle Disease	Newcastle Disease Virus (NDV)	Hemagglutination inhibition (HI) assay, Agar Gel Immunodiffusion (AGID), ELISA, RT-PCR	Highly sensitive and selective	AuNP	Purified NDV	40 nm AuNP conjugated with anti-NDV-6C4 mAb	2×10^{-12} M	171
Ebola	Ebola Virus (EBOV)	Whole antigen ELISA, Virus isolation in cell culture	Sensitive with prolonged time consuming	AuNP	EBOV Glycoprotein ($EBOV-GP_{1-649}$)	Anti-human IgG conjugated AuNP	Sensitivity: 100% Selectivity: 98%	172
				Fe_3O_4 MNPs	EBOV glycoprotein (EBOV-GP)	Anti EBOV-GP (4G7) conjugated MNPs	1 ng/ml	173

Norovirus	Norovirus	Microscopy, ELISA, RT-PCR	Reduced clinical specificity, expensive	Biotin labelled anti-Norovirus antibodies linked with streptavidin-biotin conjugated AviTag M13 phage with HRP/anti-M13 antibody	Virus-like particles (VLPs) from GI.1 (first recognized Norovirus)	Biotin labelled anti-Norovirus antibodies linked with streptavidin-biotin conjugated AviTag M13 phage with HRP/anti-M13 antibody	10^7 VLPs/ml	[174]
Dengue, Zika	DENV and Zika virus (ZIKV)	PCR amplification of specific genes, virus isolation culture, ELISA	Hard to distinguish from each other based on isolation and ELISA, expensive, cross reactivity with other viruses of Flaviviridae family	AuNS with 1,2-bis(4-pyridyl)ethylene (BPE) and 4-mercaptobenzoic acid (MBA) as Raman reporter	DENV-NS1 ZIKV-NS1	Anti-DENV NS1 and anti-ZIKV NS1 conjugated gold nanostars with different Raman reporters	DENV- 7.67 ng/ml ZIKV- 0.72 ng/ml	[43]

				AuNP	DENV-NS1 ZIKV-NS1	serotype-specific DENV nanoparticle-mAb conjugates and ZIKV nanoparticle-mAb conjugates	Sensitivity/specificity: 0.76 to 1.00 for DENV 1–4 and the pan-DENV; 0.81/0.86 for ZIKV respectively	[175]
AIDS, Hepatitis C, Hepatitis A	HIV, HCV, HAV	ELISA, Viral Load Test, Quantitative PCR, Liver Biopsy	Co-infection of HIV and HCV	AuNP	Proteinticles (P) P_{HIV}- gp41, p24 P_{HCV}- 511p, c100p, c22p, and c33c P_{HAV}- E1, E2, E3	Protein-A conjugated AuNP	Sensitivity: 100%	[176]
Dengue, Yellow Fever, Zika	DENV, Yellow Fever Virus (YFV), ZIKV			AgNP	DENV NS1 protein, Yellow Fever Virus NS1 protein, and EBOV, Zaire strain glycoprotein GP	AgNP conjugated anti-dengue NS1, anti-YFV NS1, anti-EBOV GP mAb	150 ng/ml	[177]
Kaposi's sarcoma-associated herpesvirus	HSV, *Bartonella* sp			AuNP modified with MGITC as Raman reporter (Raman-active	DNA sequences associated with KSHV and BA	Thiol modified DNA conjugated SERS active	KSHV: 0.043 pM and BA: 0.074 pM	[178]

(KSHV) and Bacillary Angiomatosis (BA)				probe)		AuNPs		

View Article Online
DOI: 10.1039/C8AN00307F

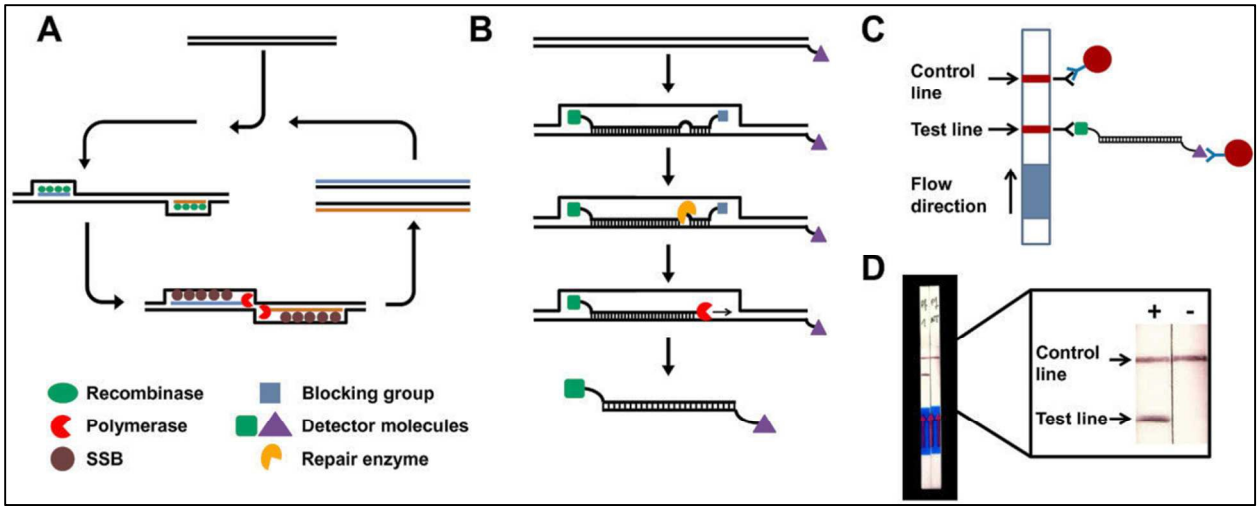

Figure-8: Schematic representation of RPA mediated LFIA device A. Reaction principle, B. Modified probe labelling, C. Detection mechanism, D. Observation of positive and negative result. Reprinted (adapted) with permission from [179]. Copyright (2014) BioMed Central Limited.

3.2 LFIA for detecting protozoal infection

Nanoparticle labelled simple lateral flow-based tool can identify labels of whole pathogen. For example, commercially available rapid test strips for malaria detection are capable of detecting *P. falciparum* and other *Plasmodium* species at levels of ≤ 500 parasites/µL and ≤ 5000 parasites/µL respectively. Also, as per WHO guidelines, some rapid test strips are available for use in the market (CareStart™ Malaria test, OptiMAL-IT™) which can detect *Plasmodium* very efficiently with parasitemias of ≥ 100 parasites/µL [120]. In other standard rapid diagnostic tests, *P. falciparum* dehydrogenase and Histidine-rich Protein 2 (*pf*HRP II) are used as species specific markers for *P. falciparum* [180]. OptiMAL-IT™ design is based on the detection of pLDH (Plasmodium lactate dehydrogenase) using pan-specific-anti-pLDH-mAbs labelled with AuNP [181]. A NTA functionalised gold and AgNP has recently been exploited for the detection of *pf*HRP II mimics specifically without any cross reactivity with human serum proteins. NTA is a chelating agent which has a high affinity towards histidine (Dissociation constant (K_d) value is in micromolar range [182]). At a low pH, NTA NPs do not show aggregation with human serum proteins which enables it for further development to detect *pf*HRP-II in human serum or saliva [121]. On the other hand, nucleic acid based lateral flow assay

View Article Online
DOI: 10.1039/C8AN00307F

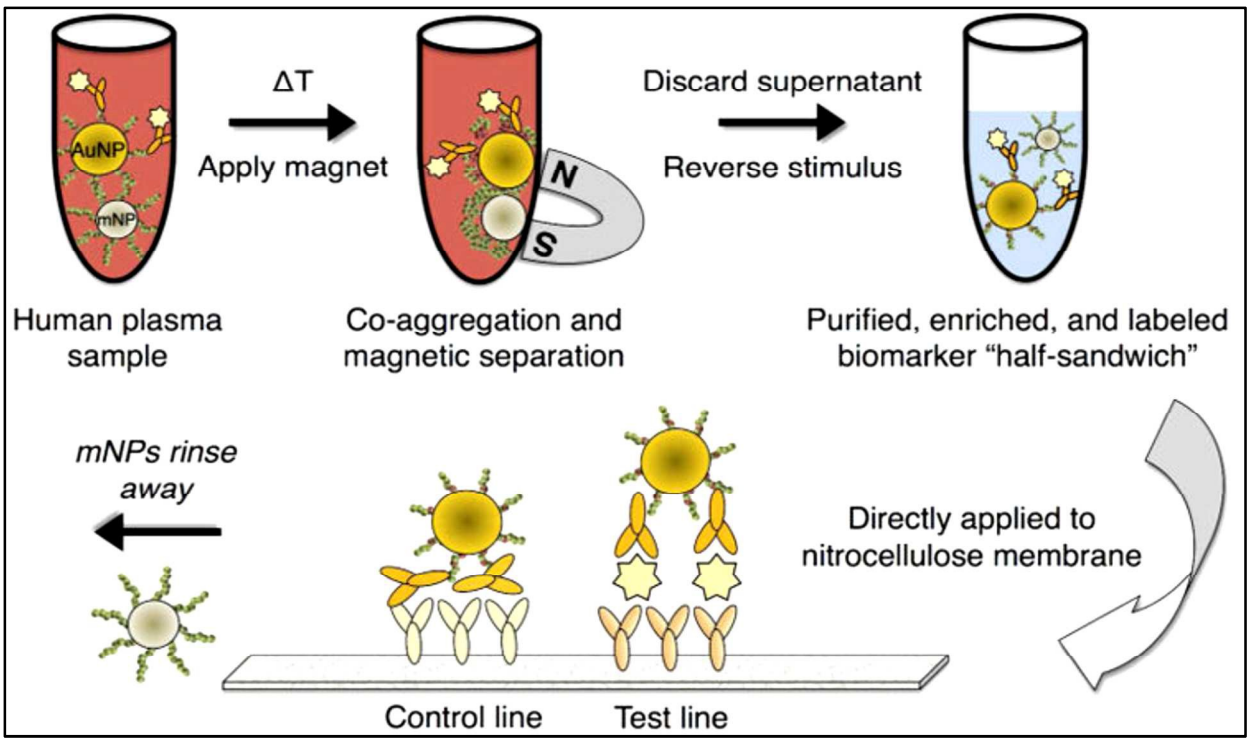

Figure-9: Schematic diagram of Magnetic enrichment LFIA. Reprinted (adapted) with permission from [122]. Copyright (2012) American Chemical Society.

for detecting malaria is also been widely studied [180].Recombinase polymerase amplification (RPA) strategy has also been used to design LFIA device. The RPA amplicon is labelled for the detection by tag-specific antibody in control and test line. The conjugate pad contains the AuNPs for visualizing colour formation (Fig-8). This gives high species-specific result with high sensitivity and specificity (100%). The detection limit was found to be 100 fg of genomic *P. falciparum* DNA (equivalent to a sensitivity of 4 parasites per reaction) [179]. Thermally responsive MNP is also being used in studies to concentrate and aggregate more amount of *pf*HRP II as a pre-step before putting the sample on the strip (Fig-9). Here, the sample was treated with biotinylated antibody which forms aggregation when treated with heat after addition of streptavidin-pNIPAm-AuNP, pNIPAm MNP and free pNIPAm polymer. The sample was then subjected to magnetic field for separating out the mixed AuNP/MNP aggregates and re-dissolved in a cold buffer for enrichment [122]. 10 ng/mL of pfHRP-II detection was achieved using this method of enrichment. A very recent report on pLDH detection using LFIA platform has successfully implemented Google Analytics platform by using QR barcode for positive, negative

View Article Online
DOI: 10.1039/C8AN00307F

and invalid results from the device (Fig-10). The cross-platform data acquisition can store a very large amount of data from the device readable by a smartphone [123]. The QR codes are initially set as "Blank" with both the QR codes incomplete (deactivated). When the test result is positive, negative or invalid, it will produce three different types of QR code which can be scanned using a smartphone camera to obtain data about the test.

Schistosomiasis is a parasite disease caused by *Schistosoma*, a blood-dwelling fluke worm [183]. UCP has been employed for detection of Circulating Anodic Antigen (CAA), a biomarker of *Schistosoma*. The detection limit achieved by using UCP was 0.5 pg/mL of CAA [126] and the robustness of the same method was improved by using dry (lyophilized) reagents with a detection limit of 30 pg/mL [127].

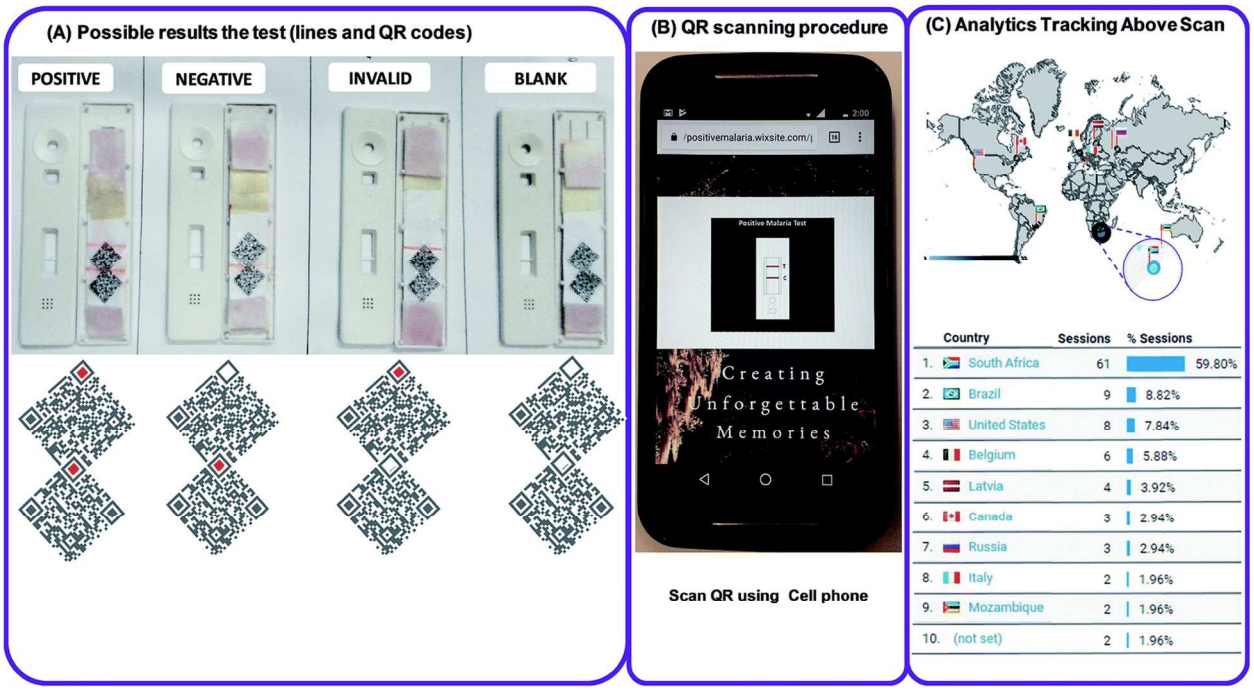

Figure-10 (A) QR code generation for positive, negative, blank and invalid tests. (B) QR scanning procedure by using cell phone (C) Statistical Google Analytics real-time data with details like number of users, location, duration, results (positive, negative or invalid) etc. Reprinted (adapted) with permission from [123]. Copyright (2017) Royal Society of Chemistry.

View Article Online
DOI: 10.1039/C8AN00307F

3.3 LFIA for detecting viruses and viral infections

Some other remarkable studies demonstrated detection of virus and viral protein using LFIA device. H9 subtype of AIV was successfully detected using LFIA strip developed using two different mAbs for test line and control line separately with a sensitivity of 0.25 Hemagglutinin units in less than 10 minutes. The antibody (4C4) against HA was labeled with AuNP and antibody (4D4) against nucleoprotein was applied on the test line [128]. Similar type of approach has been used to detect H5 subtype (H5N1) without any cross reactivity with H1-H4 or H6-H14 subtypes [184]. In comparison with Hemagglutination (HI) assay and Agar Gel Immunodiffusion Assay (AGID), the gold-immunochromatographic (GICA) test strip has shown high sensitivity and specificity [185]. Rapid detection of HBV and HEV [138] is largely constituted by immunochromatography assay principle. There are various commercial kits available for HBV, HEV rapid detection (like ACON, Atlas Medical, Dima, Cortez, Blue, Intec, HEPACARD, Assure) [136, 137, 186, 187]. They provided excellent screening with comparable sensitivity and specificity with PCR [188]. The sensitivity and specificity both ranging 97.5-98.3% had been observed with 240 patient serum sample. Use of fluorescent QDs as labels are advantageous as they have high quantum yield, tuneable fluorescent emission spectra and greater lifetime. Carboxyl modified CdSe/ZnS quantum beads (QBs) as labels had shown detection limit of hepatitis-B surface antigen (HBsAg) in picograms/mL range [142]. The detection platform comprised of anti-HBsAg mAbs conjugated with QBs. The detection limit achieved by this method was 75 pg/mL.

View Article Online
DOI: 10.1039/C8AN00307F

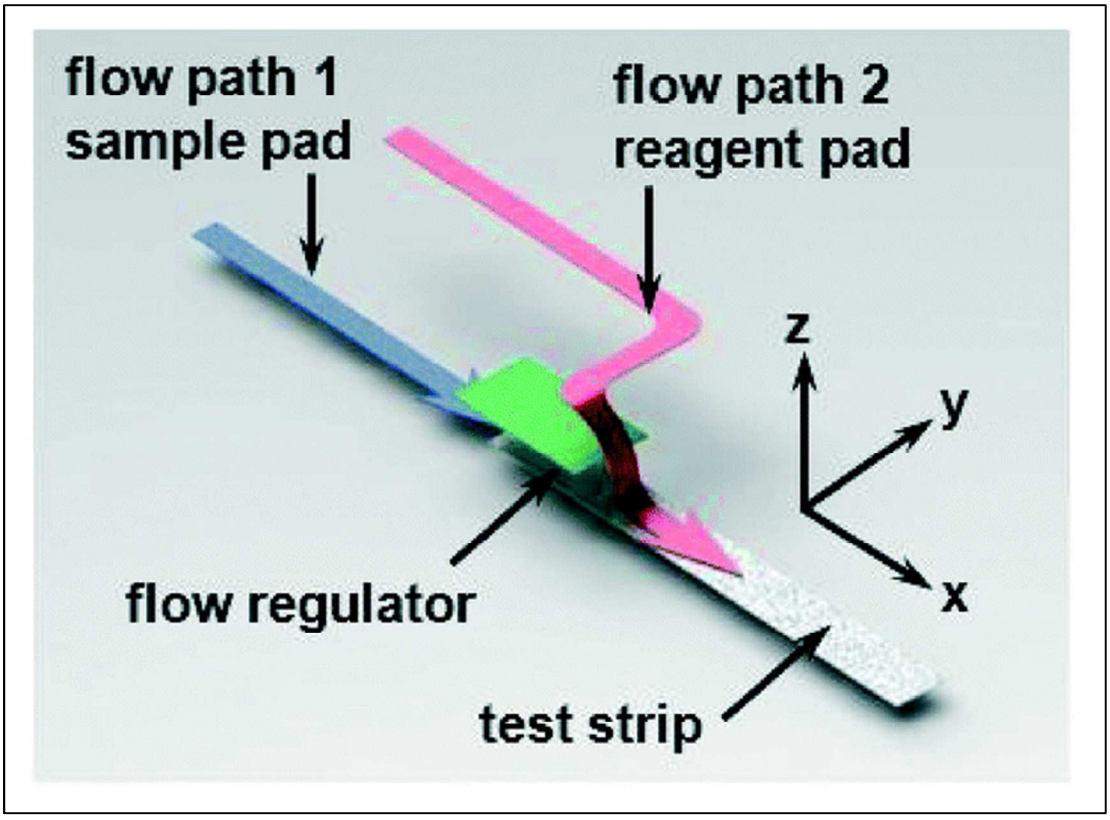

Figure-11: Schematic illustration of the stacking flow immunoassay device. Reprinted (adapted) with permission from [164] . Copyright (2015) Royal Society of Chemistry.

Several LFIA devices are designed to detect DENV in blood or saliva samples. Commercial kits for detecting DENV is designed a) to detect dengue antigen NS1 at the early stages of infection (Panbio Dengue Early Rapid NS1, SD Bioline Dengue NS1 Ag, BIORAD Strip) b) the detection of anti-dengue IgM and IgG (Panbio Dengue Duo Cassette and SD Dengue IgG/IgM, Merlin IgM, Biosynex IgM, Merlin Dengue Fever IgG and IgM combo device) or c) both antigen and IgG/IgM (BIOLINE Dengue Duo NS1antigen and IgG and IgM Combo Device) [156-163]. For improving the specificity and sensitivity of the test, several other approaches have been implemented. Detection of dengue specific IgG in salivary fluid using stacking flow platform has enabled detection of DENV in a completely non-invasive sample collection platform (Fig-11) [164]. As it is shown in the Fig-10, the device is fabricated using two flow paths, one is called sample pad and another one is reagent pad. The sample pad was introduced with spiked salivary samples and the reagent pad is supplied with protein-G conjugated 40 nm AuNPs. On the other

View Article Online
DOI: 10.1039/C8AN00307F

hand, specific detection of anti-dengue IgM from blood sample has been achieved by using a protein-G coated membrane which selectively eliminate IgG from the sample [189]. Chikungunya is another viral disease that are predominantly seen around the world over the years [190-192]. SD Bioline Chikungunya IgM and OnSite Chikungunya IgM Combo Rapid Test are two commercially available immunochromatography based lateral flow devices that have been approved by European Commission. Both of these LFIA devices are designed to detect chikungunya specific IgM present in blood and recombinant structural proteins from chikungunya envelope are conjugated with colloidal gold particles for detection. SD Bioline Chikungunya IgM have been tested with 407 samples with a sensitivity and specificity of 97.1% and 98.9% respectively [165] whereas OnSite Chikungunya IgM Combo Rapid Test showed 90.3% sensitivity and 100% specificity (both are relative to MAC-ELISA results) with 93 samples [166]. Surprisingly, multiple field studies have been conducted based on these two LFIA devices showed very poor performances [167-169, 193]. The first EBOV outbreak took place in West Africa in 2014 [194] with a fatality rate of 70.8% [195]. Rapid diagnosis of EBOV by using LFIA as a POC tool has shown 100% sensitive detection of IgG antibodies against EBOV Glycoprotein (EBOV-GP_{1-649}) [172]. A detection limit of 1ng/ml of EBOV-GP has been achieved by using Fe_3O_4 MNPs conjugated anti EBOV-GP (4G7) [173].Recently a multiplexed disease diagnostic strip has been designed to detect three different type of viruses causing Dengue, Yellow fever and Ebola [177]. The label used in this study was AgNPs of three different sizes having different colors. These nanoparticles were conjugated to antibodies specific for a particular disease was used for three different test lines to easily identify the specific virus present in the sample with a detection limit of 150 ng/ml (Fig-12). Multiplexed as well as SERS based enhanced detection of Dengue NS1 antigen and Zika NS1 antigen has also been investigated. Very low detection limit of 7.67 ng/mL and 0.72 ng/mL for DENV NS1 and ZIKV NS1 respectively has been achieved by using two different Raman reporters conjugated gold nanostars [43]. Detection of rabies virus in rabies endemic countries often lack the infrastructure and funds to employ the gold standard for definitive diagnosis of rabies infection: Fluorescent Antibody Test (FAT) [196]. For low-cost and rapid detection of rabies infection, two types of immunochromatography test kits were developed by using mAbs which can recognize epitope II and III of the nucleoprotein of the virus [197]. The specificity and sensitivity for type 1 (a single mAb

View Article Online
DOI: 10.1039/C8AN00307F

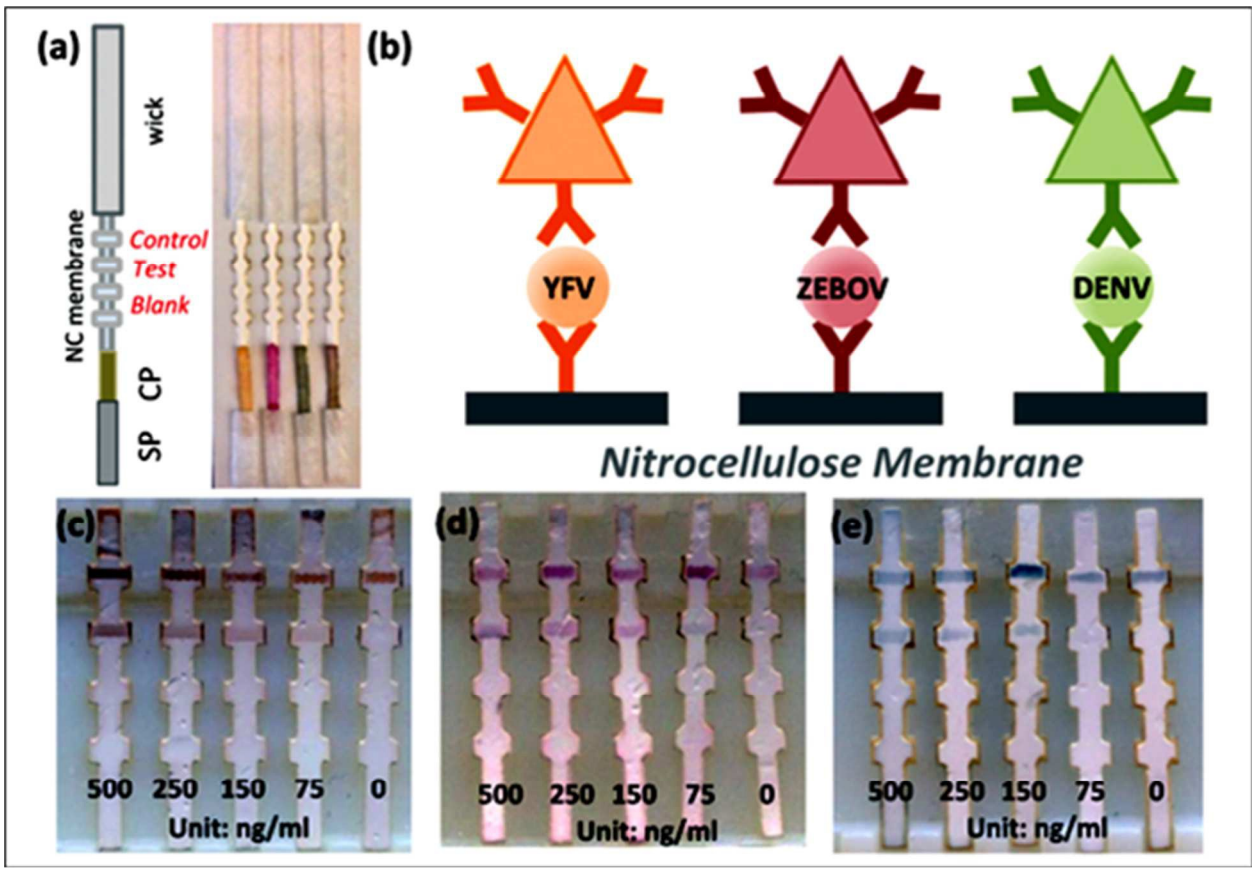

Figure-12: a. Lateral Flow Strip, b. Schematic of sandwich assay showing different colored antibodies conjugated with mAbs specific to YFV NS1, ZEBOV GP, DENV NS1 (from left to right), c-e. Limit of Detection of LFIA strip. Reprinted (adapted) with permission from [177]. Copyright (2015) Royal Society of Chemistry.

was used) and type 2 (two different mAbs were used) were found out to be 88.9%, 95.5% and 100%, 93.2% respectively. Furthermore, the assay has showed no cross reactivity with other common canine-pathogenic viruses. Commercially available immunochromatography strip for rabies virus detection has been evaluated and the specificity and sensitivity were found out to be 100% and 91.66% respectively with brain samples from different rabies suspected animals [198-201].

As per WHO, around 30% of the HIV affected people are unaware of their infectious status. Critical gaps exist in many developing countries in HIV prevention, diagnosis and treatment [202]. For that, in low resource settings, LFIA devices as a POC tool can serve this gap by providing faster and simpler detection platforms. WHO criteria for using such POC must meet the

View Article Online
DOI: 10.1039/C8AN00307F

ASSURED (Affordable, Sensitivity and Specificity, User-friendly, Rapid and robust, Equipment-free, Deliverable) requirement [203]. Determine HIV-1/2 (Abbott Laboratories) is a commercially available selenium colloid based immunochromatographic rapid test strip which uses sandwich format to detect anti-HIV-1 or anti-HIV-2 antibody present in the patient's serum or plasma or from the whole blood sample [204]. The test was evaluated by various groups. Samples from various locations around the world were tested and it correctly predicted the results from the samples with a 100% sensitivity [205-207]. Alere Determine HIV-1/2 Ag/Ab Combo is FDA approved rapid LFIA strip which is used commercially for HIV diagnosis [208]. The principle is same as that of the previously described (Determine HIV-1/2 by Abbott Laboratories) with the difference only in the analyte; here the analyte is p24 antigen as well as antibodies to HIV-1 and HIV-2 [143]. Some of the other commercially available HIV detection kits have also been evaluated and in most of the cases the sensitivity was found to be nearly 100% with serum or plasma cell [145, 206, 207, 209-211]. HIV-1 p24 detection by Magnetic Immuno Chromatographic Test (MICT) by using superparamagnetic nanoparticle [212] is also reported [144, 213]. The magnetic moment of the superparamagnetic particles which served as a label for the assay has been detected using cost-effective instrument which involves multiple coil sensors arranged as a gradiometer to form a dedicated magnetic assay reader system [144]. A recent report on detection of p24, has shown use of PtNCs which serve as catalyst in the LFIA platform. The signal amplification by using this method has shown a 100-fold catalytic enhancement and thus be able to detect 0.8 pg/ml of p24 [148] Amplified HIV-1 RNA detection [145] by NALFIA using AuNPs with resolution of 10.5-13 $\log_{10}$ copies/mL over a linear range and 50 copies of HIV *gag* RNA when coupled with Nucleic Acid Sequence Based Amplification (NASBA) [146]. The assay is designed to detect an amplified 142 bp RNA sequence by AuNP labelled partly complementary nucleotide strand. When a sample containing the RNA sequence is present, it binds with the AuNP labelled probe as well as with nucleotide sequence present in the nitrocellulose membrane of the strip. After washing the strip, gold enhancement is done for signal amplification and improving LOD (Fig-13). SERS based enhancement has been done for HIV nucleic acid detection. A detection limit as low as 0.24 pg/mL for HIV-1 DNA has been achieved by using MGITC modified AuNSs as probe [150].. Some opportunistic infection of HIV like Cryptococcosis caused by *Cryptococcus* sp. was also diagnosed and evaluated using LFIA [8, 214].

View Article Online
DOI: 10.1039/C8AN00307F

A significant cause of diseases in respiratory tract and eye (Pharyngoconjunctival fever) is Human Adenovirus. Adenovirus antigen immunochromatographic test is being developed which can detect the virus within 10 minutes from pharyngeal swap specimen [151]. The IC test showed a sensitivity of 72.6% and a specificity of 100% with serotypes 1, 2, 3, 5, 7. Other studies have also showed comparable sensitivity with the previous results [215, 216]. Another mosquito-borne virus, Western Nile Virus is a human neuropathogen commonly found in Africa, Asia, Europe and Middle East [217, 218]. Though there are many immunofluorescence assays and MAC-ELISA based techniques are available for laboratory screening of WNV, it shows 4 to 10% of cross reactivity with other flaviviruses [219-221]. A solid phase immunochromatographic strip with colloidal gold particle as label RapidWN^{TM} was developed in 2007 [154]. The LFIA showed a high sensitivity and selectivity of 98.8% and 95.3% respectively which is comparable with the gold standard IgM based EIA [155]. NDV belongs to the family of *Paramyxoviridae* family. LFIA device for detection of NDV has been achieved by using 40 nm AuNP conjugated with anti-NDV-6C4 mAb [171]. Gold enhancement on immobilized AuNP-antibody conjugate showed increased detection limit by 10-100 folds. An unconventional method to detect Norovirus used M13 bacteriophage nanoparticles as reporters instead of colored latex or AuNPs. Here, the M13 bacteriophage has been used to selectively bind to biotin labelled anti-norovirus antibodies by biotin-streptavidin-biotin conjugation. Then the horseradish peroxidase (HRP) conjugated anti-M13 antibody binds to the bacteriophage. TMB is used then as chromogenic substance to develop color [174]. The detection limit achieved by using this system was 10^7 VLPs/ml.

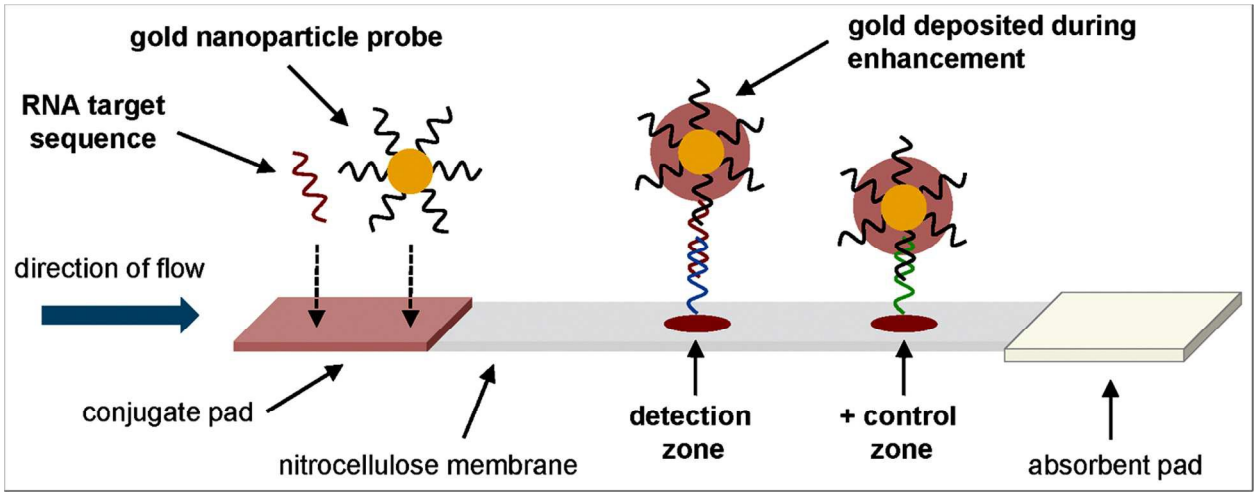

View Article Online
DOI: 10.1039/C8AN00307F

Figure-13: Schematic design of lateral flow assay to detect amplified HIV-1 RNA. Reprinted (adapted) with permission from [146]. Copyright (2012) Public Library of Sciences (PLOS).

Over the years, LFIA devices are improved by various means such as by using two-dimensional paper flow network [222, 223], installing Organic Light Emitting Diode (OLED) with filters [224], multiplexing the assay with two or more analytes [225], hand held devices (including smartphone apps) for quantitative detection of analytes [100, 123], enzyme based signal amplification [148] and gold or silver based signal amplification [132, 152, 226]. The two-dimensional paper flow system has shown controlled release from the patterned, dried reagents which allowed fabrication and implementation of complex and multiplexed flow patterns (like flow of reagents for gold enhancement) which must not mix with each other before flowing through the strip by capillary action [222]. These amplification strategies were applied to improve sensitivity of the detection device. Further, sensitivity for the detection of fluorescence coming from QD labels was improved through the use of OLED. It enabled certain advantages over conventional LEDs such as flexibility and with 7 times improvement over the conventional LFIA device in detection of influenza as a proof of concept [224].

View Article Online
DOI: 10.1039/C8AN00307F

4. Conclusion and Outlook

This review summarizes analysis and diagnosis of infectious diseases by LFIA with nanoparticles used as label. We have seen various pandemics and epidemics around the globe caused by various infectious diseases. So, it is of prior importance to diagnose infectious diseases and their causative agents as early as possible. This not only leads to the deployment of early preventive measures but also help to contain the infection from spreading. Different methods can detect either these infections causing pathogens or their products in which lateral flow assay approach provides several advantages. This method of diagnosis is simple, rapid, cost effective and does not need any specialised person or training to be operated thus serving as a point of care (POC) testing device. Different labels are used of which colloidal AuNP as primary label for visualising and/or quantifying the infection load. AuNP is comparatively easy to prepare, stable and can be readily tuned depending upon the type of application. Another advantage of lateral flow assay is different analytes can be tested at the same time which makes LFIA devices multiparametric. Several LFIA based devices are commercialised for the diagnosis of infectious disease and further extensive research is underway to enhance the signal produced from the device with several techniques like silver enhancement, SERS, magnetic enrichment etc.

Although LFIA devices are having great application, there are still some limitations associated with LFIA based devices. Selectivity and signal generation of these devices often hugely depends on the type of sample, its condition and preparation, volume of the sample, pH, amount of analyte present, weak interaction forces between the analyte and recognition element. Some of the strategies described here are experimented only with target analyte in controlled condition. This may affect the outcome of the device's performance in real samples from a patient. To overcome this, present research is focussed more on to make LFIA devices more feasible, less dependent on sample preparation processes, shorter incubation time and quantitative result generation. Further, for analytes, that are present in very low concentration in the sample of interest, a pre-concentration or enrichment step is generally performed. This makes LFIA not suitable for POC applications. To overcome this hurdle, methods such as catalytic enhancement and SERS based detection are being employed to achieve better sensitivity.

View Article Online
DOI: 10.1039/C8AN00307F

List of acronyms:

AgNP(s) – Silver nanoparticles(s)

AIDS – Acquired Immunodeficiency Syndrome

AIV – Avian Influenza Virus

AuNP(s) – Gold nanoparticle(s)

BoNT (A/B/C/D/E) – Botulinum Neurotoxin (A/B/C/D/E)

CAA - Circulating Anodic Antigen

CFU – Colony Forming Unit

CNP(s) – Carbon nanoparticles(s)

CPS – Capsular Polysaccharide

DENV – Dengue Virus

ds – Double Stranded

EBOV – Ebola Virus

EHEC - Enterohemorrhagic *E. coli*

EIA – Enzyme Immunoassay

ELISA - Enzyme-Linked Immunosorbent Assay

EPEC – Enteropathogenic *E. coli*

FAT - Fluorescent Antibody Test

GO – Graphene Oxide

H(A/B/C/E)V – Hepatitis (A/B/C/E) Virus

HA - Hemagglutinin

HBeAg – Hepatitis B Envelope Antigen

HBsAg - Hepatitis B Surface Antigen

View Article Online
DOI: 10.1039/C8AN00307F

HI – Hemagglutinin Inhibition

HIV – Human Immunodeficiency Virus

HRP - Horseradish Peroxidase

HSV - Herpes Simplex Virus

IMP – Immunomagnetic Particle

IMS – Immuno-Magnetic Separation

LFIA – Lateral Flow Immuno Assay

LPS – Lipo-polysaccharide

mAb(s) – Monoclonal Antibody(ies)

MAC – IgM Antibody Capture

MB – Methylene Blue

MNB – Magnetic Nano-Beads

MNP(s) - Magnetic Nanoparticle(s)

mRNA – Messenger RNA

NALFIA- Nucleic Acid Lateral Flow Immuno Assay

NASBA - Nucleic Acid Sequence Based Amplification

NDV – Newcastle Disease Virus

NTA - Ni(II)-nitrilotriacetic acid

ODN – Oligodinucleotide

pAb - Polyclonal Antibody

PCR - Polymerase Chain Reaction

PEG – Poly(ethylene glycol)

pf HRP – *Plasmodium falciparum* Histidine Rich Protein

View Article Online
DOI: 10.1039/C8AN00307F

PFU – Plaque Forming Unit

PIF – Powdered Infant Formulae

pLDH – *Plasmodium* Lactate Dehydrogenase

pNIPAM - Poly(*N*-isopropylacrylamide)

POC – Point of Care

QD(s) – Quantum Dot(s)

QR – Quick Response

r-DNA/RNA – Recombinant DNA/RNA

RNALFIA – Ribonucleic Acid LFIA

RT-LAMP - Reverse-Transcription Loop-Mediated Isothermal Amplification

SEB – *Staphylococcus* enterotoxin B

SERS – Surface Enhanced Raman Scattering

SRB - Sulforhodamine B

ss – Single Stranded

ss DNA – single stranded DNA

TCID - Tissue Culture Infectious Dose

UCP – Up-converting Phosphor

VLP(s) – Virus Like Particle(s)

WHO – World Health Organization

YFV – Yellow Fever Virus

ZIKV – Zika Virus

Acknowledgements

View Article Online
DOI: 10.1039/C8AN00307F

The authors acknowledge the support from BioX centre, Indian Institute of Technology Mandi for research and infrastructure facility. RB acknowledges the fellowship from MHRD, Govt of India.

References

1. J. H. Leuvering, P. J. Thal, M. van der Waart and A. H. Schuurs, *J Immunoassay*, 1980, **1**, 77-91.
2. E. C. Schramm, N. R. Staten, Z. Zhang, S. S. Bruce, C. Kellner, J. P. Atkinson, V. C. Kyttaris, G. C. Tsokos, M. Petri, E. Sander Connolly and P. K. Olson, *Anal Biochem*, 2015, **477**, 78-85.
3. N. De Giovanni and N. Fucci, *Curr Med Chem*, 2013, **20**, 545-561.
4. R. Pacifici, M. Farre, S. Pichini, J. Ortuno, P. N. Roset, P. Zuccaro, J. Segura and R. de la Torre, *J Anal Toxicol*, 2001, **25**, 144-146.
5. A. Carrio, C. Sampedro, J. L. Sanchez-Lopez, M. Pimienta and P. Campoy, *Sensors (Basel)*, 2015, **15**, 29569-29593.
6. R. Kwizera, J. Nguna, A. Kiragga, J. Nakavuma, R. Rajasingham, D. R. Boulware and D. B. Meya, *PLoS One*, 2014, **9**, e103156.
7. S. Buhrer-Sekula, H. L. Smits, G. C. Gussenhoven, J. van Leeuwen, S. Amador, T. Fujiwara, P. R. Klatser and L. Oskam, *J Clin Microbiol*, 2003, **41**, 1991-1995.
8. J. N. Jarvis, A. Percival, S. Bauman, J. Pelfrey, G. Meintjes, G. N. Williams, N. Longley, T. S. Harrison and T. R. Kozel, *Clin Infect Dis*, 2011, **53**, 1019-1023.
9. M. L. Moreno, A. Cebolla, A. Munoz-Suano, C. Carrillo-Carrion, I. Comino, A. Pizarro, F. Leon, A. Rodriguez-Herrera and C. Sousa, *Gut*, 2017, **66**, 250-257.
10. V. S. Vaidya, G. M. Ford, S. S. Waikar, Y. Wang, M. B. Clement, V. Ramirez, W. E. Glaab, S. P. Troth, F. D. Sistare, W. C. Prozialeck, J. R. Edwards, N. A. Bobadilla, S. C. Mefferd and J. V. Bonventre, *Kidney Int*, 2009, **76**, 108-114.
11. S. H. Ang, M. Rambeli, T. M. Thevarajah, Y. B. Alias and S. M. Khor, *Biosens Bioelectron*, 2016, **78**, 187-193.

View Article Online
DOI: 10.1039/C8AN00307F

12. R. E. Biagini, D. L. Sammons, J. P. Smith, B. A. MacKenzie, C. A. Striley, J. E. Snawder, S. A. Robertson and C. P. Quinn, *Clin Vaccine Immunol*, 2006, **13**, 541-546.
13. S. Rosen, in *Lateral Flow Immunoassay*, eds. R. C. Wong and H. Y. Tse, Springer, New York, 2009, ch. 2, pp. 35-50.
14. X. Huang, Z. P. Aguilar, H. Xu, W. Lai and Y. Xiong, *Biosens Bioelectron*, 2016, **75**, 166-180.
15. K. M. Koczula and A. Gallotta, *Essays Biochem*, 2016, **60**, 111-120.
16. World Health Organization . 2015, https://books.google.co.in/books?hl=en&lr=&id=Kl00DgAAQBAJ&oi=fnd&pg=PP1&dq=World+Health+Organization.+2015.+Mortality+and+global+health+estimates.+Geneva,+Switzerland:+World+Health+Organization&ots=8MrFnAPOwc&sig=2XZQEy7SlofM3888phKwJSe_dgc#v=onepage&q&f=false Mortality and global health estimates. Geneva, Switzerland: World Health Organization, (accessed January 2018).
17. C. Dye, *Philos Trans R Soc Lond B Biol Sci*, 2014, **369**, 20130426.
18. G. A. Posthuma-Trumpie, J. Korf and A. van Amerongen, *Anal Bioanal Chem*, 2009, **393**, 569-582.
19. G. A. Posthuma-Trumpie, J. H. Wichers, M. Koets, L. B. Berendsen and A. van Amerongen, *Anal Bioanal Chem*, 2012, **402**, 593-600.
20. Y. Xu, Y. Liu, Y. Wu, X. Xia, Y. Liao and Q. Li, *Anal Chem*, 2014, **86**, 5611-5614.
21. D. Quesada-Gonzalez and A. Merkoci, *Biosens Bioelectron*, 2015, **73**, 47-63.
22. E. B. Bahadır and M. K. Sezgintürk, *TrAC Trends in Analytical Chemistry*, 2016, **82**, 286-306.
23. M. J. Raeisossadati, N. M. Danesh, F. Borna, M. Gholamzad, M. Ramezani, K. Abnous and S. M. Taghdisi, *Biosens Bioelectron*, 2016, **86**, 235-246.
24. K. Wang, W. Qin, Y. Hou, K. Xiao and W. Yan, *Nano Biomed Eng*, 2016, **8**, 172-183.
25. X. Gong, J. Cai, B. Zhang, Q. Zhao, J. Piao, W. Peng, W. Gao, D. Zhou, M. Zhao and J. Chang, *Journal of Materials Chemistry B*, 2017, **5**, 5079-5091.
26. M. Sajid, A.-N. Kawde and M. Daud, *Journal of Saudi Chemical Society*, 2015, **19**, 689-705.
27. B. Ngom, Y. Guo, X. Wang and D. Bi, *Anal Bioanal Chem*, 2016, **408**, 3923.

View Article Online
DOI: 10.1039/C8AN00307F

28. J. Y. Lee, Y. A. Kim, M. Y. Kim, Y. T. Lee, B. D. Hammock and H. S. Lee, *Anal Chim Acta*, 2012, **757**, 69-74.

29. Rapid Lateral Flow Test Strips: Considerations for Product Development, Merck Millipore, Billerica https://www.emdmillipore.com/Web-US-Site/en_CA/-/USD/ShowDocument-Pronet?id=201306.12550 (accessed March, 2018).

30. I. H. Cho, S. M. Seo, E. H. Paek and S. H. Paek, *J Chromatogr B Analyt Technol Biomed Life Sci*, 2010, **878**, 271-277.

31. P. F. Mens, A. van Amerongen, P. Sawa, P. A. Kager and H. D. Schallig, *Diagn Microbiol Infect Dis*, 2008, **61**, 421-427.

32. Z. Wang, D. Zhi, Y. Zhao, H. Zhang, X. Wang, Y. Ru and H. Li, *Int J Nanomedicine*, 2014, **9**, 1699-1707.

33. S. Takanashi, M. Okame, T. Shiota, M. Takagi, F. Yagyu, P. G. Tung, S. Nishimura, N. Katsumata, T. Igarashi, S. Okitsu and H. Ushijima, *J Virol Methods*, 2008, **148**, 1-8.

34. J. S. Ponti, in *Lateral Flow Immunoassay*, eds. R. C. Wong and H. Y. Tse, Springer, New York, 2009, ch. 2, pp. 35-50.

35. A. van Amerongen, D. van Loon, L. B. Berendsen and J. H. Wichers, *Clin Chim Acta*, 1994, **229**, 67-75.

36. J. A. Ho and M. R. Huang, *Anal Chem*, 2005, **77**, 3431-3436.

37. E. R. Goldman, A. R. Clapp, G. P. Anderson, H. T. Uyeda, J. M. Mauro, I. L. Medintz and H. Mattoussi, *Anal Chem*, 2004, **76**, 684-688.

38. P. Corstjens, M. Zuiderwijk, A. Brink, S. Li, H. Feindt, R. S. Niedbala and H. Tanke, *Clin Chem*, 2001, **47**, 1885-1893.

39. Y. C. Cao, R. Jin and C. A. Mirkin, *Science*, 2002, **297**, 1536-1540.

40. J. Hwang, S. Lee and J. Choo, *Nanoscale*, 2016, **8**, 11418-11425.

41. L. Blanco-Covian, V. Montes-Garcia, A. Girard, M. T. Fernandez-Abedul, J. Perez-Juste, I. Pastoriza-Santos, K. Faulds, D. Graham and M. C. Blanco-Lopez, *Nanoscale*, 2017, **9**, 2051-2058.

42. O. J. Clarke, B. L. Goodall, H. P. Hui, N. Vats and C. L. Brosseau, *Anal Chem*, 2017, **89**, 1405-1410.

43. M. Sanchez-Purra, M. Carre-Camps, H. de Puig, I. Bosch, L. Gehrke and K. Hamad-Schifferli, *ACS Infect Dis*, 2017, **3**, 767-776.

View Article Online
DOI: 10.1039/C8AN00307F

44. P. Sandström, M. Boncheva and B. Åkerman, *Langmuir*, 2003, **19**, 7537-7543.
45. J. M. de la Fuente and S. Penades, *Biochim Biophys Acta*, 2006, **1760**, 636-651.
46. S. Zeng, K.-T. Yong, I. Roy, X.-Q. Dinh, X. Yu and F. Luan, *Plasmonics*, 2011, **6**, 491.
47. A. K. Gupta and M. Gupta, *Biomaterials*, 2005, **26**, 3995-4021.
48. B. Pelaz, P. del Pino, P. Maffre, R. Hartmann, M. Gallego, S. Rivera-Fernandez, J. M. de la Fuente, G. U. Nienhaus and W. J. Parak, *ACS Nano*, 2015, **9**, 6996-7008.
49. A. K. Gupta, R. R. Naregalkar, V. D. Vaidya and M. Gupta, *Nanomedicine*, 2007, **2**, 23-39.
50. P. C. Soo, Y. T. Horng, P. R. Hsueh, B. J. Shen, J. Y. Wang, H. H. Tu, J. R. Wei, S. C. Hsieh, C. C. Huang and H. C. Lai, *J Microbiol Methods*, 2006, **66**, 440-448.
51. K. A. Edwards and A. J. Baeumner, *Anal Bioanal Chem*, 2006, **386**, 1335-1343.
52. B. Y. Jung, S. C. Jung and C. H. Kweon, *J Food Prot*, 2005, **68**, 2140-2143.
53. J. Wang, W. N. Chen, K. X. Hu and W. Li, *Wei Sheng Yan Jiu*, 2006, **35**, 439-441.
54. H. Qi, Z. Zhong, H. X. Zhou, C. Y. Deng, H. Zhu, J. F. Li, X. L. Wang and F. R. Li, *Int J Nanomedicine*, 2011, **6**, 3033-3039.
55. Q. Y. Xie, Y. H. Wu, Q. R. Xiong, H. Y. Xu, Y. H. Xiong, K. Liu, Y. Jin and W. H. Lai, *Biosens Bioelectron*, 2014, **54**, 262-265.
56. J. Park, J. H. Shin and J. K. Park, *Anal Chem*, 2016, **88**, 3781-3788.
57. E. Morales-Narvaez, T. Naghdi, E. Zor and A. Merkoci, *Anal Chem*, 2015, **87**, 8573-8577.
58. K. H. Seo, P. S. Holt, H. D. Stone and R. K. Gast, *Int J Food Microbiol*, 2003, **87**, 139-144.
59. Z. Fang, W. Wu, X. Lu and L. Zeng, *Biosens Bioelectron*, 2014, **56**, 192-197.
60. C.-C. Liu, C.-Y. Yeung, P.-H. Chen, M.-K. Yeh and S.-Y. Hou, *Food Chemistry*, 2013, **141**, 2526-2532.
61. S. Rong-Hwa, T. Shiao-Shek, C. Der-Jiang and H. Yao-Wen, *Food Chemistry*, 2010, **118**, 462-466.
62. M. Fisher, Y. Atiya-Nasagi, I. Simon, M. Gordin, A. Mechaly and S. Yitzhaki, *Lett Appl Microbiol*, 2009, **48**, 413-418.
63. D. B. Wang, B. Tian, Z. P. Zhang, J. Y. Deng, Z. Q. Cui, R. F. Yang, X. Y. Wang, H. P. Wei and X. E. Zhang, *Biosens Bioelectron*, 2013, **42**, 661-667.

View Article Online
DOI: 10.1039/C8AN00307F

64. D. B. Wang, B. Tian, Z. P. Zhang, X. Y. Wang, J. Fleming, L. J. Bi, R. F. Yang and X. E. Zhang, *Biosens Bioelectron*, 2015, **67**, 608-614.

65. N. Nakasone, C. Toma, Y. Lu and M. Iwanaga, *Diagn Microbiol Infect Dis*, 2007, **57**, 21-25.

66. K. Kawatsu, Y. Kumeda, M. Taguchi, W. Yamazaki-Matsune, M. Kanki and K. Inoue, *J Clin Microbiol*, 2008, **46**, 1226-1231.

67. L. Yu, P. Li, X. Ding and Q. Zhang, *Talanta*, 2017, **165**, 167-175.

68. D. Tang, J. C. Sauceda, Z. Lin, S. Ott, E. Basova, I. Goryacheva, S. Biselli, J. Lin, R. Niessner and D. Knopp, *Biosens Bioelectron*, 2009, **25**, 514-518.

69. Y.-M. Huang, D.-F. Liu, W.-H. Lai, Y.-H. Xiong, W.-C. Yang, K. Liu and S.-Y. Wang, *Chinese Journal of Analytical Chemistry*, 2014, **42**, 654-659.

70. D. Liu, Y. Huang, S. Wang, K. Liu, M. Chen, Y. Xiong, W. Yang and W. Lai, *Food Control*, 2015, **51**, 218-224.

71. L. Anfossi, F. Di Nardo, S. Cavalera, C. Giovannoli, G. Spano, E. S. Speranskaya, I. Y. Goryacheva and C. Baggiani, *Microchimica Acta*, 2018, **185**, 94.

72. T. Klewitz, F. Gessler, H. Beer, K. Pflanz and T. Scheper, *Sensors and Actuators B: Chemical*, 2006, **113**, 582-589.

73. D. J. Chiao, J. J. Wey, R. H. Shyu and S. S. Tang, *Hybridoma (Larchmt)*, 2008, **27**, 31-35.

74. K. H. Ching, A. Lin, J. A. McGarvey, L. H. Stanker and R. Hnasko, *J Immunol Methods*, 2012, **380**, 23-29.

75. S.-H. Huang, H.-C. Wei and Y.-C. Lee, *Food Control*, 2007, **18**, 893-897.

76. S.-H. Huang, *Sensors and Actuators B: Chemical*, 2007, **127**, 335-340.

77. S. Wiriyachaiporn, P. H. Howarth, K. D. Bruce and L. A. Dailey, *Diagn Microbiol Infect Dis*, 2013, **75**, 28-36.

78. N. Khreich, P. Lamourette, H. Boutal, K. Devilliers, C. Creminon and H. Volland, *Anal Biochem*, 2008, **377**, 182-188.

79. Y. Ju, H. J. Hao, G. H. Xiong, H. R. Geng, Y. L. Zheng, J. Wang, Y. Cao, Y. H. Yang, X. H. Cai and Y. Q. Jiang, *Vet Immunol Immunopathol*, 2010, **133**, 207-211.

View Article Online
DOI: 10.1039/C8AN00307F

80. T. Nakayama, J. Zhao, D. Takeuchi, A. Kerdsin, P. Chiranairadul, P. Areeratana, P. Loetthong, A. Pienpringam, Y. Akeda and K. Oishi, *Biosens Bioelectron*, 2014, **60**, 175-179.

81. X. Zhang, J. Zhou, C. Zhang, D. Zhang and X. Su, *RSC Advances*, 2016, **6**, 1279-1287.

82. M. Blazkova, B. Javurkova, L. Fukal and P. Rauch, *Biosens Bioelectron*, 2011, **26**, 2828-2834.

83. H. L. Smits, C. K. Eapen, S. Sugathan, M. Kuriakose, M. H. Gasem, C. Yersin, D. Sasaki, B. Pujianto, M. Vestering, T. H. Abdoel and G. C. Gussenhoven, *Clin Diagn Lab Immunol*, 2001, **8**, 166-169.

84. A. B. Nurul Najian, E. A. Engku Nur Syafirah, N. Ismail, M. Mohamed and C. Y. Yean, *Anal Chim Acta*, 2016, **903**, 142-148.

85. C. Y. Yu, G. Y. Ang, A. L. Chua, E. H. Tan, S. Y. Lee, G. Falero-Diaz, O. Otero, I. Rodriguez, F. Reyes, A. Acosta, M. E. Sarmiento, S. Ghosh, T. Ramamurthy, C. Yean Yean, P. Lalitha and M. Ravichandran, *J Microbiol Methods*, 2011, **86**, 277-282.

86. C. Pengsuk, P. Chaivisuthangkura, S. Longyant and P. Sithigorngul, *Biosens Bioelectron*, 2013, **42**, 229-235.

87. L. Wang, J. Zhang, H. Bai, X. Li, P. Lv and A. Guo, *Applied Biochemistry and Biotechnology*, 2014, **173**, 1073-1082.

88. A. J. Herring, R. C. Ballard, V. Pope, R. A. Adegbola, J. Changalucha, D. W. Fitzgerald, E. W. Hook, A. Kubanova, S. Mananwatte, J. W. Pape, A. W. Sturm, B. West, Y. P. Yin and R. W. Peeling, *Sexually Transmitted Infections*, 2006, **82**, v7-v12.

89. P. Mdluli, P. Tetyana, N. Sosibo, H. van der Walt, M. Mlambo, A. Skepu and R. Tshikhudo, *Biosens Bioelectron*, 2014, **54**, 1-6.

90. H. Liu, F. Zhan, F. Liu, M. Zhu, X. Zhou and D. Xing, *Biosens Bioelectron*, 2014, **62**, 38-46.

91. M. Blažková, M. Koets, P. Rauch and A. van Amerongen, *European Food Research and Technology*, 2009, **229**, 867.

92. Z. Lin, S. Cheng, Q. Yan, X. Liu, W. Zheng, X. Hu, J. Li, J. Zhang, T. Xiang, J. Zheng and J. Zhang, *Clin Biochem*, 2015, **48**, 1298-1303.

93. F. Chen, X. Ming, X. Chen, M. Gan, B. Wang, F. Xu and H. Wei, *Biosens Bioelectron*, 2014, **61**, 306-313.

View Article Online
DOI: 10.1039/C8AN00307F

94. J. A. Ho, S. C. Zeng, W. H. Tseng, Y. J. Lin and C. H. Chen, *Anal Bioanal Chem*, 2008, **391**, 479-485.

95. S. Xia, Z. Yu, D. Liu, C. Xu and W. Lai, *Food Control*, 2016, **59**, 507-512.

96. Q. Qu, Z. Zhu, Y. Wang, Z. Zhong, J. Zhao, F. Qiao, X. Du, Z. Wang, R. Yang, L. Huang, Y. Yu, L. Zhou and Z. Chen, *J Microbiol Methods*, 2009, **79**, 121-123.

97. F. Zhang, M. Zou, Y. Chen, J. Li, Y. Wang, X. Qi and Q. Xue, *Biosens Bioelectron*, 2014, **51**, 29-35.

98. Z. Liang, X. Wang, W. Zhu, P. Zhang, Y. Yang, C. Sun, J. Zhang, X. Wang, Z. Xu, Y. Zhao, R. Yang, S. Zhao and L. Zhou, *ACS Appl Mater Interfaces*, 2017, **9**, 3497-3504.

99. C. Z. Li, K. Vandenberg, S. Prabhulkar, X. Zhu, L. Schneper, K. Methee, C. J. Rosser and E. Almeide, *Biosens Bioelectron*, 2011, **26**, 4342-4348.

100. J. H. Shin, J. Hong, H. Go, J. Park, M. Kong, S. Ryu, K. P. Kim, E. Roh and J. K. Park, *J Agric Food Chem*, 2018, **66**, 290-297.

101. S. Shafazand, R. Doyle, S. Ruoss, A. Weinacker and T. A. Raffin, *Chest*, 1999, **116**, 1369-1376.

102. Z. A. Kanafani, A. Ghossain, A. I. Sharara, J. M. Hatem and S. S. Kanj, *Emerg Infect Dis*, 2003, **9**, 520-525.

103. L. W. Riley, R. S. Remis, S. D. Helgerson, H. B. McGee, J. G. Wells, B. R. Davis, R. J. Hebert, E. S. Olcott, L. M. Johnson, N. T. Hargrett, P. A. Blake and M. L. Cohen, *N Engl J Med*, 1983, **308**, 681-685.

104. W. Wu, S. Zhao, Y. Mao, Z. Fang, X. Lu and L. Zeng, *Analytica Chimica Acta*, 2015, **861**, 62-68.

105. C. Pohlmann, I. Dieser and M. Sprinzl, *Analyst*, 2014, **139**, 1063-1071.

106. R. V. Tauxe, C. M. Patton, P. Edmonds, T. J. Barrett, D. J. Brenner and P. A. Blake, *J Clin Microbiol*, 1985, **21**, 222-225.

107. J. Singh, S. Sharma and S. Nara, *Food Chem*, 2015, **170**, 470-483.

108. H. D. Shukla and S. K. Sharma, *Crit Rev Microbiol*, 2005, **31**, 11-18.

109. S. S. Arnon, R. Schechter, T. V. Inglesby, D. A. Henderson, J. G. Bartlett, M. S. Ascher, E. Eitzen, A. D. Fine, J. Hauer, M. Layton, S. Lillibridge, M. T. Osterholm, T. O'Toole, G. Parker, T. M. Perl, P. K. Russell, D. L. Swerdlow, K. Tonat and B. Working Group on Civilian, *JAMA*, 2001, **285**, 1059-1070.

View Article Online
DOI: 10.1039/C8AN00307F

110. J. Kadariya, T. C. Smith and D. Thapaliya, *Biomed Res Int*, 2014, **2014**, 827965.
111. M. C. Heidt, W. Mohamed, T. Hain, P. R. Vogt, T. Chakraborty and E. Domann, *J Clin Microbiol*, 2005, **43**, 4898-4901.
112. S. Sriskandan and J. D. Slater, *PLoS Med*, 2006, **3**, e187.
113. X. Jiang, Y. Ni, Y. Jiang, F. Yuan, L. Han, M. Li, H. Liu, L. Yang and Y. Lu, *J Clin Microbiol*, 2005, **43**, 826-831.
114. M. L. Mezzatesta, F. Gona and S. Stefani, *Future Microbiol*, 2012, **7**, 887-902.
115. R. Chauhan, J. Singh, T. Sachdev, T. Basu and B. D. Malhotra, *Biosens Bioelectron*, 2016, **81**, 532-545.
116. S. Shan, W. Lai, Y. Xiong, H. Wei and H. Xu, *J Agric Food Chem*, 2015, **63**, 745-753.
117. A.-L. Välimaa, A. Tilsala-Timisjärvi and E. Virtanen, *Food Control*, 2015, **55**, 103-114.
118. X. Wang, R. Niessner, D. Tang and D. Knopp, *Anal Chim Acta*, 2016, **912**, 10-23.
119. T. Yang, H. Huang, F. Zhu, Q. Lin, L. Zhang and J. Liu, *Sensors (Basel)*, 2016, **16**.
120. A. Ratsimbasoa, A. Randriamanantena, R. Raherinjafy, N. Rasoarilalao and D. Menard, *Am J Trop Med Hyg*, 2007, **76**, 481-485.
121. J. D. Swartz, C. P. Gulka, F. R. Haselton and D. W. Wright, *Langmuir*, 2011, **27**, 15330-15339.
122. M. A. Nash, J. N. Waitumbi, A. S. Hoffman, P. Yager and P. S. Stayton, *ACS Nano*, 2012, **6**, 6776-6785.
123. C. L. Mthembu, M. I. Sabela, M. Mlambo, L. M. Madikizela, S. Kanchi, H. Gumede and P. S. Mdluli, *Analytical Methods*, 2017, **9**, 5943-5951.
124. D. Y. Pereira, R. Y. Chiu, S. C. Zhang, B. M. Wu and D. T. Kamei, *Anal Chim Acta*, 2015, **882**, 83-89.
125. L. Rivas, A. de la Escosura-Muñiz, L. Serrano, L. Altet, O. Francino, A. Sánchez and A. Merkoçi, *Nano Research*, 2015, **8**, 3704-3714.
126. P. L. Corstjens, L. van Lieshout, M. Zuiderwijk, D. Kornelis, H. J. Tanke, A. M. Deelder and G. J. van Dam, *J Clin Microbiol*, 2008, **46**, 171-176.
127. G. J. van Dam, C. J. de Dood, M. Lewis, A. M. Deelder, L. van Lieshout, H. J. Tanke, L. H. van Rooyen and P. L. Corstjens, *Exp Parasitol*, 2013, **135**, 274-282.
128. F. Peng, Z. Wang, S. Zhang, R. Wu, S. Hu, Z. Li, X. Wang and D. Bi, *Clin Vaccine Immunol*, 2008, **15**, 569-574.

View Article Online
DOI: 10.1039/C8AN00307F

129. V. Veguilla, K. Hancock, J. Schiffer, P. Gargiullo, X. Lu, D. Aranio, A. Branch, L. Dong, C. Holiday, F. Liu, E. Steward-Clark, H. Sun, B. Tsang, D. Wang, M. Whaley, Y. Bai, L. Cronin, P. Browning, H. Dababneh, H. Noland, L. Thomas, L. Foster, C. P. Quinn, S. D. Soroka and J. M. Katz, *J Clin Microbiol*, 2011, **49**, 2210-2215.

130. Y. T. Kim, J. H. Jung, Y. K. Choi and T. S. Seo, *Biosens Bioelectron*, 2014, **61**, 485-490.

131. J. H. Jung, S. J. Oh, Y. T. Kim, S. Y. Kim, W. J. Kim, J. Jung and T. S. Seo, *Anal Chim Acta*, 2015, **853**, 541-547.

132. K. Mitamura, H. Shimizu, M. Yamazaki, M. Ichikawa, K. Nagai, J. Katada, A. Wada, C. Kawakami and N. Sugaya, *J Virol Methods*, 2013, **194**, 123-128.

133. N. Wiriyachaiporn, W. Maneeprakorn, C. Apiwat and T. Dharakul, *Microchimica Acta*, 2015, **182**, 85-93.

134. T. T. Le, P. Chang, D. J. Benton, J. W. McCauley, M. Iqbal and A. E. G. Cass, *Anal Chem*, 2017, **89**, 6781-6786.

135. S. Bamrungsap, C. Apiwat, W. Chantima, T. Dharakul and N. Wiriyachaiporn, *Microchimica Acta*, 2014, **181**, 223-230.

136. D. T. Lau, H. Ma, S. M. Lemon, E. Doo, M. G. Ghany, E. Miskovsky, G. L. Woods, Y. Park and J. H. Hoofnagle, *J Viral Hepat*, 2003, **10**, 331-334.

137. K. S. Myint, M. Guan, H. Y. Chen, Y. Lu, D. Anderson, T. Howard, H. Noedl and M. P. Mammen, Jr., *Am J Trop Med Hyg*, 2005, **73**, 942-946.

138. H. Y. Chen, Y. Lu, T. Howard, D. Anderson, P. Y. Fong, W. P. Hu, C. P. Chia and M. Guan, *Clin Diagn Lab Immunol*, 2005, **12**, 593-598.

139. T. Salminen, E. Juntunen, N. Khanna, K. Pettersson and S. M. Talha, *J Virol Methods*, 2016, **228**, 67-73.

140. L. Li, L. Zhou, Y. Yu, Z. Zhu, C. Lin, C. Lu and R. Yang, *Diagn Microbiol Infect Dis*, 2009, **63**, 165-172.

141. S. Huaibin, Y. Hang, N. Jin Zhong, X. Shasha, Z. Changhua, M. Lan and L. Lin Song, *Nanotechnology*, 2011, **22**, 375602.

142. J. Shen, Y. Zhou, F. Fu, H. Xu, J. Lv, Y. Xiong and A. Wang, *Talanta*, 2015, **142**, 145-149.

View Article Online
DOI: 10.1039/C8AN00307F

143. US Food and Drug Administration, https://www.fda.gov/downloads/biologicsbloodvaccines/bloodbloodproducts/approvedproducts/premarketapprovalspmas/ucm364698.pdf, (accessed January 2018).
144. S. Workman, S. K. Wells, C. P. Pau, S. M. Owen, X. F. Dong, R. LaBorde and T. C. Granade, *J Virol Methods*, 2009, **160**, 14-21.
145. H. H. Lee, M. A. Dineva, Y. L. Chua, A. V. Ritchie, I. Ushiro-Lumb and C. A. Wisniewski, *J Infect Dis*, 2010, **201 Suppl 1**, S65-72.
146. B. A. Rohrman, V. Leautaud, E. Molyneux and R. R. Richards-Kortum, *PLoS One*, 2012, **7**, e45611.
147. Z. A. Parpia, R. Elghanian, A. Nabatiyan, D. R. Hardie and D. M. Kelso, *JAIDS Journal of Acquired Immune Deficiency Syndromes*, 2010, **55**, 413-419.
148. C. N. Loynachan, M. R. Thomas, E. R. Gray, D. A. Richards, J. Kim, B. S. Miller, J. C. Brookes, S. Agarwal, V. Chudasama, R. A. McKendry and M. M. Stevens, *ACS Nano*, 2018, **12**, 279-288.
149. J. Hu, L. Wang, F. Li, Y. L. Han, M. Lin, T. J. Lu and F. Xu, *Lab Chip*, 2013, **13**, 4352-4357.
150. X. Fu, Z. Cheng, J. Yu, P. Choo, L. Chen and J. Choo, *Biosens Bioelectron*, 2016, **78**, 530-537.
151. H. Tsutsumi, K. Ouchi, M. Ohsaki, T. Yamanaka, Y. Kuniya, Y. Takeuchi, C. Nakai, H. Meguro and S. Chiba, *J Clin Microbiol*, 1999, **37**, 2007-2009.
152. A. Wada, Y. Sakoda, T. Oyamada and H. Kida, *J Virol Methods*, 2011, **178**, 82-86.
153. X. Li, D. Lu, Z. Sheng, K. Chen, X. Guo, M. Jin and H. Han, *Talanta*, 2012, **100**, 1-6.
154. N. A. Shaikh, J. Ge, Y. X. Zhao, P. Walker and M. Drebot, *Clin Chem*, 2007, **53**, 2031-2034.
155. A. R. Sambol and S. H. Hinrichs, *J Virol Methods*, 2009, **157**, 223-226.
156. S. D. Blacksell, J. A. Doust, P. N. Newton, S. J. Peacock, N. P. Day and A. M. Dondorp, *Trans R Soc Trop Med Hyg*, 2006, **100**, 775-784.
157. S. D. Blacksell, P. N. Newton, D. Bell, J. Kelley, M. P. Mammen, Jr., D. W. Vaughn, V. Wuthiekanun, A. Sungkakum, A. Nisalak and N. P. Day, *Clin Infect Dis*, 2006, **42**, 1127-1134.

View Article Online
DOI: 10.1039/C8AN00307F

158. T. T. Nga, K. T. Thai, H. L. Phuong, P. T. Giao, Q. Hung le, T. Q. Binh, V. T. Mai, N. Van Nam and P. J. de Vries, *Clin Vaccine Immunol*, 2007, **14**, 799-801.

159. P. Dussart, L. Petit, B. Labeau, L. Bremand, A. Leduc, D. Moua, S. Matheus and L. Baril, *PLoS Negl Trop Dis*, 2008, **2**, e280.

160. M. Moorthy, S. Chandy, K. Selvaraj and A. M. Abraham, *Indian J Med Microbiol*, 2009, **27**, 254-256.

161. R. Lima Mda, R. M. Nogueira, H. G. Schatzmayr and F. B. dos Santos, *PLoS Negl Trop Dis*, 2010, **4**, e738.

162. L. Osorio, M. Ramirez, A. Bonelo, L. A. Villar and B. Parra, *Virol J*, 2010, **7**, 361.

163. V. Tricou, H. T. Vu, N. V. Quynh, C. V. Nguyen, H. T. Tran, J. Farrar, B. Wills and C. P. Simmons, *BMC Infect Dis*, 2010, **10**, 142.

164. Y. Zhang, J. Bai and J. Y. Ying, *Lab Chip*, 2015, **15**, 1465-1471.

165. MD Doctors Direct, http://www.mddoctorsdirect.com/sites/default/files/product-pdf/46FK10_Chikungunya-IgM(D)_CE(Rev.4).pdf, (accessed January 2018).

166. CTKbiotech Online, http://ctkbiotech.com/ctk-product/chikungunya-igm-combo-rapid-test-ce/, (accessed January 2018).

167. S. D. Blacksell, A. Tanganuchitcharnchai, R. G. Jarman, R. V. Gibbons, D. H. Paris, M. S. Bailey, N. P. Day, R. Premaratna, D. G. Lalloo and H. J. de Silva, *Clin Vaccine Immunol*, 2011, **18**, 1773-1775.

168. H. Kosasih, S. Widjaja, E. Surya, S. H. Hadiwijaya, D. P. Butarbutar, U. A. Jaya, Nurhayati, B. Alisjahbana and M. Williams, *Southeast Asian J Trop Med Public Health*, 2012, **43**, 55-61.

169. C. M. Prat, O. Flusin, A. Panella, B. Tenebray, R. Lanciotti and I. Leparc-Goffart, *Emerg Infect Dis*, 2014, **20**, 2129-2132.

170. E. I. Laderman, E. Whitworth, E. Dumaual, M. Jones, A. Hudak, W. Hogrefe, J. Carney and J. Groen, *Clin Vaccine Immunol*, 2008, **15**, 159-163.

171. J. Li, M. Zou, Y. Chen, Q. Xue, F. Zhang, B. Li, Y. Wang, X. Qi and Y. Yang, *Anal Chim Acta*, 2013, **782**, 54-58.

172. P. Brangel, A. Sobarzo, C. Parolo, B. S. Miller, P. D. Howes, S. Gelkop, J. J. Lutwama, J. M. Dye, R. A. McKendry, L. Lobel and M. M. Stevens, *ACS Nano*, 2018, **12**, 63-73.

View Article Online
DOI: 10.1039/C8AN00307F

173. D. Duan, K. Fan, D. Zhang, S. Tan, M. Liang, Y. Liu, J. Zhang, P. Zhang, W. Liu, X. Qiu, G. P. Kobinger, G. F. Gao and X. Yan, *Biosens Bioelectron*, 2015, **74**, 134-141.

174. A. E. Hagstrom, G. Garvey, A. S. Paterson, S. Dhamane, M. Adhikari, M. K. Estes, U. Strych, K. Kourentzi, R. L. Atmar and R. C. Willson, *PLoS One*, 2015, **10**, e0126571.

175. I. Bosch, H. de Puig, M. Hiley, M. Carre-Camps, F. Perdomo-Celis, C. F. Narvaez, D. M. Salgado, D. Senthoor, M. O'Grady, E. Phillips, A. Durbin, D. Fandos, H. Miyazaki, C. W. Yen, M. Gelvez-Ramirez, R. V. Warke, L. S. Ribeiro, M. M. Teixeira, R. P. Almeida, J. E. Munoz-Medina, J. E. Ludert, M. L. Nogueira, T. E. Colombo, A. C. B. Terzian, P. T. Bozza, A. S. Calheiros, Y. R. Vieira, G. Barbosa-Lima, A. Vizzoni, J. Cerbino-Neto, F. A. Bozza, T. M. L. Souza, M. R. O. Trugilho, A. M. B. de Filippis, P. C. de Sequeira, E. T. A. Marques, T. Magalhaes, F. J. Diaz, B. N. Restrepo, K. Marin, S. Mattar, D. Olson, E. J. Asturias, M. Lucera, M. Singla, G. R. Medigeshi, N. de Bosch, J. Tam, J. Gomez-Marquez, C. Clavet, L. Villar, K. Hamad-Schifferli and L. Gehrke, *Sci Transl Med*, 2017, **9**.

176. J. H. Lee, H. S. Seo, J. H. Kwon, H. T. Kim, K. C. Kwon, S. J. Sim, Y. J. Cha and J. Lee, *Biosens Bioelectron*, 2015, **69**, 213-225.

177. C. W. Yen, H. de Puig, J. O. Tam, J. Gomez-Marquez, I. Bosch, K. Hamad-Schifferli and L. Gehrke, *Lab Chip*, 2015, **15**, 1638-1641.

178. X. Wang, N. Choi, Z. Cheng, J. Ko, L. Chen and J. Choo, *Analytical Chemistry*, 2017, **89**, 1163-1169.

179. S. Kersting, V. Rausch, F. F. Bier and M. von Nickisch-Rosenegk, *Malar J*, 2014, **13**, 99.

180. M. S. Cordray and R. R. Richards-Kortum, *Am J Trop Med Hyg*, 2012, **87**, 223-230.

181. A. H. Moody and P. L. Chiodini, *British journal of biomedical science*, 2002, **59**, 228-231.

182. S. Knecht, D. Ricklin, A. N. Eberle and B. Ernst, *J Mol Recognit*, 2009, **22**, 270-279.

183. B. Gryseels, K. Polman, J. Clerinx and L. Kestens, *Lancet*, 2006, **368**, 1106-1118.

184. S. Cui and G. Tong, *J Vet Diagn Invest*, 2008, **20**, 567-571.

185. D. Peng, S. Hu, Y. Hua, Y. Xiao, Z. Li, X. Wang and D. Bi, *Vet Immunol Immunopathol*, 2007, **117**, 17-25.

186. D. H. Whang and T. Um, *The Korean Journal of Laboratory Medicine*, 2005, **25**, 186-191.

View Article Online
DOI: 10.1039/C8AN00307F

187. Y. Khudyakov and S. Kamili, *Virus Res*, 2011, **161**, 84-92.

188. M. H. K. Ansari, M. D. Omrani and V. Movahedi, *Hepat Mon*, 2007, **7**, 87-91.

189. P. Yager, E. Fu, T. Liang, B. Lutz and J. L. Osborn, 2011.

190. G. Rezza, L. Nicoletti, R. Angelini, R. Romi, A. C. Finarelli, M. Panning, P. Cordioli, C. Fortuna, S. Boros, F. Magurano, G. Silvi, P. Angelini, M. Dottori, M. G. Ciufolini, G. C. Majori, A. Cassone and C. s. group, *Lancet*, 2007, **370**, 1840-1846.

191. F. Staikowsky, F. Talarmin, P. Grivard, A. Souab, I. Schuffenecker, K. Le Roux, M. Lecuit and A. Michault, *PLoS One*, 2009, **4**, e7603.

192. W. Van Bortel, F. Dorleans, J. Rosine, A. Blateau, D. Rousset, S. Matheus, I. Leparc-Goffart, O. Flusin, C. Prat, R. Cesaire, F. Najioullah, V. Ardillon, E. Balleydier, L. Carvalho, A. Lemaitre, H. Noel, V. Servas, C. Six, M. Zurbaran, L. Leon, A. Guinard, J. van den Kerkhof, M. Henry, E. Fanoy, M. Braks, J. Reimerink, C. Swaan, R. Georges, L. Brooks, J. Freedman, B. Sudre and H. Zeller, *Euro Surveill*, 2014, **19**.

193. E. Burdino, G. Calleri, P. Caramello and V. Ghisetti, *Emerg Infect Dis*, 2016, **22**, 1837-1839.

194. Centers for Disease Control and Prevention https://www.cdc.gov/vhf/ebola/outbreaks/history/chronology.html (accessed January 2018)).

195. W. H. O. E. R. Team, B. Aylward, P. Barboza, L. Bawo, E. Bertherat, P. Bilivogui, I. Blake, R. Brennan, S. Briand, J. M. Chakauya, K. Chitala, R. M. Conteh, A. Cori, A. Croisier, J. M. Dangou, B. Diallo, C. A. Donnelly, C. Dye, T. Eckmanns, N. M. Ferguson, P. Formenty, C. Fuhrer, K. Fukuda, T. Garske, A. Gasasira, S. Gbanyan, P. Graaff, E. Heleze, A. Jambai, T. Jombart, F. Kasolo, A. M. Kadiobo, S. Keita, D. Kertesz, M. Kone, C. Lane, J. Markoff, M. Massaquoi, H. Mills, J. M. Mulba, E. Musa, J. Myhre, A. Nasidi, E. Nilles, P. Nouvellet, D. Nshimirimana, I. Nuttall, T. Nyenswah, O. Olu, S. Pendergast, W. Perea, J. Polonsky, S. Riley, O. Ronveaux, K. Sakoba, R. Santhana Gopala Krishnan, M. Senga, F. Shuaib, M. D. Van Kerkhove, R. Vaz, N. Wijekoon Kannangarage and Z. Yoti, *N Engl J Med*, 2014, **371**, 1481-1495.

196. H. Bourhy, P. E. Rollin, J. Vincent and P. Sureau, *J Clin Microbiol*, 1989, **27**, 519-523.

View Article Online
DOI: 10.1039/C8AN00307F

197. A. Nishizono, P. Khawplod, K. Ahmed, K. Goto, S. Shiota, K. Mifune, T. Yasui, K. Takayama, Y. Kobayashi, K. Mannen, V. Tepsumethanon, C. Mitmoonpitak, S. Inoue and K. Morimoto, *Microbiol Immunol*, 2008, **52**, 243-249.

198. B. Kang, J. Oh, C. Lee, B. K. Park, Y. Park, K. Hong, K. Lee, B. Cho and D. Song, *J Virol Methods*, 2007, **145**, 30-36.

199. S. Kasempimolporn, W. Saengseesom, S. Huadsakul, S. Boonchang and V. Sitprija, *J Vet Diagn Invest*, 2011, **23**, 1197-1201.

200. D. K. Yang, E. K. Shin, Y. I. Oh, K. W. Lee, C. S. Lee, S. Y. Kim, J. A. Lee and J. Y. Song, *J Vet Sci*, 2012, **13**, 43-48.

201. P. Sharma, C. K. Singh and D. Narang, *Vet World*, 2015, **8**, 135-138.

202. World Health Organization, http://www.who.int/hiv/topics/vct/about/en/ (accessed January, 2018)).

203. G. Wu and M. H. Zaman, *Bull World Health Organ*, 2012, **90**, 914-920.

204. H. Arai, B. Petchclai, K. Khupulsup, T. Kurimura and K. Takeda, *J Clin Microbiol*, 1999, **37**, 367-370.

205. S. Aidoo, W. K. Ampofo, J. A. Brandful, S. V. Nuvor, J. K. Ansah, N. Nii-Trebi, J. S. Barnor, F. Apeagyei, T. Sata, D. Ofori-Adjei and K. Ishikawa, *J Clin Microbiol*, 2001, **39**, 2572-2575.

206. R. Ribeiro-Rodrigues, L. Ferreira da Silva Pinto Neto, C. B. Cunha, V. P. Cabral and R. Dietze, *Clin Diagn Lab Immunol*, 2003, **10**, 303-307.

207. T. C. Granade, B. S. Parekh, P. M. Tih, T. Welty, E. Welty, M. Bulterys, G. Ndikintum, G. Nkuoh and S. Tancho, *Clin Diagn Lab Immunol*, 2005, **12**, 855-860.

208. Centers for Disease Control and Prevention https://hiv-tests-advantages-disadvantages.pdf (accessed January, 2018).

209. S. Phillips, T. C. Granade, C. P. Pau, D. Candal, D. J. Hu and B. S. Parekh, *Clin Diagn Lab Immunol*, 2000, **7**, 698-699.

210. F. Ketema, C. Zeh, D. C. Edelman, R. Saville and N. T. Constantine, *J Acquir Immune Defic Syndr*, 2001, **27**, 63-70.

211. H. Syed Iqbal, P. Balakrishnan, K. G. Murugavel and S. Suniti, *J Clin Lab Anal*, 2008, **22**, 178-185.

View Article Online
DOI: 10.1039/C8AN00307F

212. Y. Wang, H. Xu, M. Wei, H. Gu, Q. Xu and W. Zhu, *Materials Science and Engineering: C*, 2009, **29**, 714-718.

213. T. C. Granade, S. Workman, S. K. Wells, A. N. Holder, S. M. Owen and C. P. Pau, *Clin Vaccine Immunol*, 2010, **17**, 1034-1039.

214. M. D. Lindsley, N. Mekha, H. C. Baggett, Y. Surinthong, R. Autthateinchai, P. Sawatwong, J. R. Harris, B. J. Park, T. Chiller, S. A. Balajee and N. Poonwan, *Clin Infect Dis*, 2011, **53**, 321-325.

215. E. Uchio, K. Aoki, W. Saitoh, N. Itoh and S. Ohno, *Ophthalmology*, 1997, **104**, 1294-1299.

216. T. Fujimoto, T. Okafuji, T. Okafuji, M. Ito, S. Nukuzuma, M. Chikahira and O. Nishio, *J Clin Microbiol*, 2004, **42**, 5489-5492.

217. G. L. Campbell, A. A. Marfin, R. S. Lanciotti and D. J. Gubler, *Lancet Infect Dis*, 2002, **2**, 519-529.

218. K. A. Gyure, *J Neuropathol Exp Neurol*, 2009, **68**, 1053-1060.

219. P. Koraka, H. Zeller, M. Niedrig, A. D. Osterhaus and J. Groen, *Microbes Infect*, 2002, **4**, 1209-1215.

220. A. K. Malan, P. J. Stipanovich, T. B. Martins, H. R. Hill and C. M. Litwin, *Am J Clin Pathol*, 2003, **119**, 508-515.

221. A. K. Malan, T. B. Martins, H. R. Hill and C. M. Litwin, *J Clin Microbiol*, 2004, **42**, 727-733.

222. G. E. Fridley, H. Le and P. Yager, *Anal Chem*, 2014, **86**, 6447-6453.

223. J. Hu, S. Wang, L. Wang, F. Li, B. Pingguan-Murphy, T. J. Lu and F. Xu, *Biosens Bioelectron*, 2014, **54**, 585-597.

224. V. Venkatraman and A. J. Steckl, *Biosens Bioelectron*, 2015, **74**, 150-155.

225. J. Li and J. Macdonald, *Biosens Bioelectron*, 2016, **85**, 998-999.

226. X. Cao, Y. Ye and S. Liu, *Anal Biochem*, 2011, **417**, 1-16.